



Theses and Dissertations

2003-03-11

An Investigation of Compliant Over-running Ratchet and Pawl Clutches

Gregory Mark Roach
Brigham Young University - Provo

Follow this and additional works at: <https://scholarsarchive.byu.edu/etd>



Part of the [Mechanical Engineering Commons](#)

BYU ScholarsArchive Citation

Roach, Gregory Mark, "An Investigation of Compliant Over-running Ratchet and Pawl Clutches" (2003). *Theses and Dissertations*. 55.
<https://scholarsarchive.byu.edu/etd/55>

This Thesis is brought to you for free and open access by BYU ScholarsArchive. It has been accepted for inclusion in Theses and Dissertations by an authorized administrator of BYU ScholarsArchive. For more information, please contact scholarsarchive@byu.edu, ellen_amatangelo@byu.edu.

AN INVESTIGATION OF COMPLIANT OVER-RUNNING
RATCHET AND PAWL CLUTCHES

A Thesis

Presented to the

Department of Mechanical Engineering

Brigham Young University

In Partial Fulfillment

of the Requirements for the Degree

Master of Science

by

Gregory M. Roach

August 1998

This thesis by Gregory M. Roach is accepted in its present form by the Department of Mechanical Engineering of Brigham Young University as satisfying the thesis requirement for the degree of Master of Science.

Larry L. Howell, Committee Chair

Jordan J. Cox, Committee Member

Kay S. Mortensen, Committee Member

Date

Craig C. Smith, Graduate Coordinator

AN INVESTIGATION OF COMPLIANT OVER-RUNNING
RATCHET AND PAWL CLUTCHES

Gregory M. Roach

Department of Mechanical Engineering

M.S. Degree, August 1998

ABSTRACT

This thesis proposes that compliant mechanism theory can be used to design over-running ratchet and pawl clutches with reduced part count, lower assembly and manufacturing time while maintaining functionality. An extension of the theory to the micro regime is also briefly addressed. The results of the research show that the ratchet and pawl type of over-running clutch is a good choice for the use of compliance, and the clutch pawls should be loaded in compression to get the largest amount of output torque. It was found that compliant mechanism theory can be used to design ratchet and pawl clutches with fewer parts and lower manufacturing and assembly costs, and that these clutches perform comparable to traditional rigid-body ratchet and pawl clutches. Compliant ratchet and pawl clutches can replace traditional rigid-body clutches in some applications and now make it possible to be used in applications where it was once not economically feasible to use an over-running clutch. It was also found that these clutches function at the micro level.

COMMITTEE APPROVAL:

Larry L. Howell, Committee Chair

Jordan J. Cox, Committee Member

Kay S. Mortensen, Committee Member

Craig C. Smith, Graduate Coordinator

ACKNOWLEDGMENTS

This research was supported by the National Science Foundation under an NSF CAREER Award under grant No. DMI-9624574. The support of the NSF is gratefully acknowledged.

I would like to express my thanks to the College of Engineering and Technology and the Department of Mechanical Engineering for the use of their resources, especially the work stations and the prototyping mill in the graduate lab. I also greatly acknowledge the use of the resources in the Integrated Microelectronics Laboratory.

The help of Scott Lyon with the construction of the dynamic model and the help of Clint Mortensen with manufacturing and testing of the clutches is acknowledged and appreciated.

I would like to thank the members of my committee, Dr. Kay Mortensen and Dr. Jordan Cox for their help in reviewing my research and for the suggestions that have helped me to organize and focus my research in the proper direction.

I would like to especially thank my graduate advisor, Dr. Larry Howell for his patience and understanding. The many discussions we have had provided me with the needed guidance and feedback that made it possible for me to complete my research. He gave me the freedom and encouragement to pursue my ideas.

I also express my thanks to the members of the compliant mechanisms research group and those in the graduate lab for the many meetings and discussions of MEMS and

compliant mechanisms that have increased my knowledge and benefited my research and learning experience.

I acknowledge the help and guidance of my Father in Heaven. Without his help I never would have accomplished this work.

I would also like to give a special thanks to my bride Stacy for her love and support and to my parents.

TABLE OF CONTENTS

LIST OF FIGURES	viii
LIST OF TABLES	x
CHAPTER 1 Introduction.....	1
CHAPTER 2 Introduction to Overrunning Clutches	4
2.1 History of overrunning clutches	4
2.2 Types of overrunning clutches	7
2.2.1 The Spring Clutch	7
2.2.2 The Roller Clutch.....	8
2.2.3 The Sprag Clutch	9
2.2.4 The Ratchet and Pawl Clutch.....	11
CHAPTER 3 An introduction to Compliant Mechanisms.....	13
3.1 Introduction.....	13
3.2 Overrunning Clutch Comparison.....	16
3.2.1 Revolute Joints.....	16
3.2.2 Possible Part Count Reduction	16
3.2.3 Springs in the System	17
3.2.4 Joint Revolution Requirements.....	17
3.2.5 Possible Reduction in Weight	17
3.2.6 Clutch Engagement.....	18
CHAPTER 4 Compliant Mechanism Design.....	20
4.1 Introduction.....	20
4.2 Literature Review	20
4.3 The Pseudo-Rigid-Body Model	25
4.3.1 The Pseudo-rigid-body Model for Cantilever Beams.....	25
4.3.2 The pseudo-rigid-body model for initially curved cantilever beams.....	32
4.3.3 The pseudo-rigid-body model for small-length flexural pivots.....	36
CHAPTER 5 Alternative Ratchet and Pawl Clutch Designs	39
5.1 Bending Loading Designs.....	40
5.1.1 Bending Clutch Design 1	40
5.1.1.1 Test Results	43
5.1.2 Bending Clutch Design 2	43

5.1.2.1 Test Results	44
5.2 Tension Designs	45
5.2.1 Tension Clutch Design 1	45
5.2.1.1 Test Results	46
5.2.2 Tension Clutch Design 2	46
5.2.2.1 Test Results	48
5.3 Compression Designs	49
5.3.1 Compression Clutch Design 1	49
5.3.1.1 Test Results	50
5.3.2 Compression Clutch Design 2	50
5.3.3 Passive Joints	51
5.3.4 Test Results	54
 CHAPTER 6 Additional Clutch Theory	 56
6.1 Dynamic Model for Centrifugal Throw-out	56
6.1.1 Example	59
6.1.2 Test Results	60
6.2 Design of the Cam Profile for the Pawl	62
6.3 Design of Passive Joints	63
 CHAPTER 7 Clutch Design Issues	 66
7.1 Manufacturing	66
7.2 Material Selection	67
7.3 Backlash	69
7.4 Wear	70
7.5 Fatigue	71
 CHAPTER 8 Clutch Comparison and Investigation of Failure Modes	 76
8.1 Clutch Comparison	76
8.1.1 Manufacturing Time	76
8.1.2 Assembly and Part Count	77
8.1.3 Peak Static Torque	79
8.1.4 Clutch Weight	80
8.1.5 Fatigue	80
8.2 Investigation of Failure Modes	82
 CHAPTER 9 Overrunning Clutch Applications	 84
9.1 One-way Operation	84
9.2 Backstopping	85
9.3 Indexing	86

CHAPTER 10 Conclusions and Reccommendations	87
10.1 Conclusions.....	87
10.2 Reccommendations for Further Research.....	88
References.....	89
Appendix A.....	94

LIST OF FIGURES

Figure 2-1	A compliant catapult with a ratchet (Smith and Rees, 1978).	5
Figure 2-2	Schwinn 1870 free-wheeling roller clutch (Schwinn, 1945).	6
Figure 2-3	A wrapped spring clutch.	7
Figure 2-4	Typical roller clutch diagram (Stieber http:// www.riv.org/stieber.htm).	9
Figure 2-5	Typical sprag clutch diagram (Hilliard Corporation http:// www.hilliard-corp.com/images / sprag.jpg).	10
Figure 2-6	A ratchet and pawl clutch.	11
Figure 3-1	(a) A rigid-body parallel guiding mechanism and (b) a partially compliant parallel guiding mechanism.	14
Figure 3-2	A fully compliant parallel guiding mechanism.	14
Figure 3-3	A rigid-body ratchet and pawl clutch with three pawls, pin joints, and leaf springs.	19
Figure 4-1	A cantilever beam in its initial and deflected position and its corresponding pseudo-rigid-body model.	26
Figure 4-2	The pseudo-rigid-body model of a cantilever beam with applied component forces.	30
Figure 4-3	An initially curved cantilever beam in its initial and deflected positions. .	32
Figure 4-4	The Pseudo-rigid-body model of an initially curved end-loaded cantilever beam.	33
Figure 4-5	A small-length flexural pivot in its initial and deflected position and its pseudo-rigid body model.	37
Figure 5-1	A compliant ratchet and pawl clutch. The pawls are loaded in bending in the torque output direction.	41
Figure 5-2	The pseudo-rigid-body model of the cantilever beam.	41
Figure 5-3	A compliant ratchet and pawl clutch with the pawls loaded in bending. The post serves to increase the stiffness of the beam in the torque output direction by decreasing the effective length of the cantilever beam.	44
Figure 5-4	A compliant ratchet and pawl clutch with the pawls loaded in tension by the ratchet teeth.	45
Figure 5-5	A compliant ratchet and pawl overrunning clutch with small-length flexural pivots.	47
Figure 5-6	The PRBM of the small-length flexural pivot superimposed on the clutch pawl.	47
Figure 5-7	A compliant ratchet and pawl clutch with the pawls loaded in compression.	49
Figure 5-8	A compliant ratchet and pawl clutch with the pawls loaded in compression.	51
Figure 5-9	The diagram of compressive forces on the passive joint.	52
Figure 6-1	The dynamic clutch model for centrifugal throw-out of the pawls.	57
Figure 6-2	Mathematical model for centrifugal throw-out of pawls.	58

Figure 6-3	A compliant overrunning ratchet and pawl clutch with centrifugal throw-out.	60
Figure 6-4	The CAD profile of the compliant overrunning clutch with centrifugal throw-out.	61
Figure 6-5	Diagram of the cam profile, the initial contact point, and the engagement depth of the pawl tooth into a ratchet tooth,.	62
Figure 6-6	The clutch pawl shown in its normal operating position (original position) and in its deflected position for manufacturing.	65
Figure 7-1	An aluminum overrunning compliant ratchet and pawl clutch with centrifugal throw-out.	69
Figure 7-2	A compliant overrunning ratchet and pawl clutch with the pawls offset to reduce backlash.	70
Figure 7-3	S-N curve for AISI 1040 CD steel.....	74
Figure 8-1	A traditional rigid-body ratchet and pawl clutch.	77
Figure 8-2	Disassembled rigid-body ratchet and pawl clutch.	78
Figure 8-3	Disassembled compliant ratchet and pawl clutch.	78

LIST OF TABLES

Table 3-1: Clutch Type Comparison	18
Table 4-1: Values for c_{θ} for various angle of force (Howell and Midha, 1997).	29
Table 4-2: Values for γ , ρ , and K_{Θ} for differing κ_0	36
Table 5-1: Clutch Type Comparison	55
Table 7-1: Material strength to Young's modulus ratios.....	68

This thesis proposes that compliant mechanism theory can be used to design over-running ratchet and pawl clutches with reduced part count, assembly, and manufacturing time while maintaining functionality. An extension of the theory to the micro regime is also briefly addressed. The compliant over-running clutch makes it possible to expand the range of possible applications, especially those applications where it was once not economically feasible to use an over-running clutch. This is the first time that in-depth research has been done to apply compliant mechanism theory to over-running ratchet and pawl clutch design. Fatigue and wear have been identified as important design issues, but are not the focus of this research. The thesis provides an exploration of different compliant clutch designs and the necessary theory for the design of the clutch with the best performance characteristics.

The thesis will follow the organization outlined in Figure 1-1. First, a review of over-running clutch types is given in Chapter 2. This review is followed by Chapter 3 that

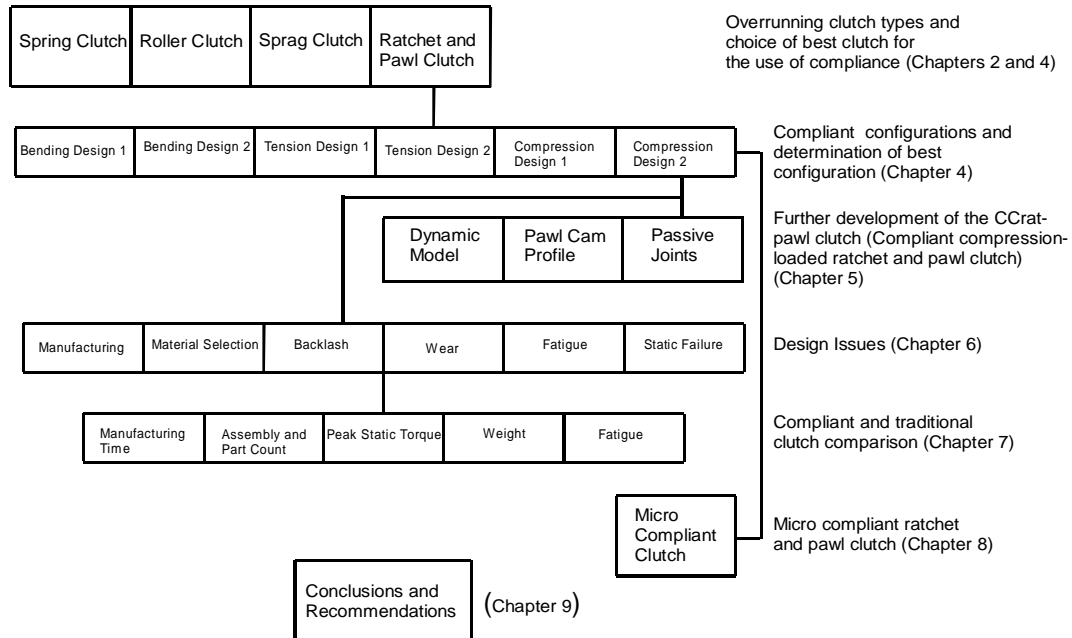


Figure 1-1 The organizational tree for the thesis.

contains an introduction to compliant mechanism theory, including the pseudo-rigid-body model, that will be used in clutch design.

Next, in Chapter 4, an examination of over-running clutches to determine the type that offers the greatest opportunity for the use of compliance is provided. A list of characteristics that make a mechanism a good candidate for the use of compliance is used to profile each type of over-running clutch. The over-running clutch type that possesses the largest amount of these characteristics is then chosen for further investigation.

Also presented in Chapter 4 are different compliant clutch designs within the chosen clutch type along with the preliminary design theory. Several candidate solutions are explored using compliant members in various configurations of tension, compression and bending loading to develop high output torque and reduce overall part count. The compliant members are designed using traditional linear deflection equations where

possible. For non-linear deflections, the pseudo-rigid-body model is used to design the compliant members. Equations are developed that relate beam stiffness to torque. After the preliminary theory and design is accomplished, the candidate solutions are prototyped and tested in order to determine the best design. Computer-aided-engineering software is used to analyze, design and create numerical tool paths to prototype the candidate clutch designs. The clutches, manufactured from polypropylene, are tested using a reaction torque sensor and a handheld strain gage to measure the output and free-wheeling torques. Polypropylene was chosen because of its material properties (a high ratio of Young's modulus to strength) which make it excellent for use in compliant mechanism design. The designs are rated on the ratio of output torque to free-wheeling torque, and the best design is the clutch with the highest rating.

As shown in the organizational tree, Chapter 5 provides the further development of the best design. The possible effects of dynamic loads are investigated and a dynamic model is created to reduce wear and noise. A proper cam profile, developed to reduce noise and wear, and a brief discussion on passive joints are also provided.

Chapter 6 contains an investigation of design issues such as manufacturing, material selection, backlash, wear, fatigue, and static failure. Possible manufacturing methods are discussed. Different material types are investigated to determine their strengths, weakness and possible uses. Clutch assembly is also examined along with fatigue. Static failure is determined by applying an overloading torque until the clutch fails. Additional investigations are done using the results from the failure investigations to make the design more robust.

Next, Chapter 7 presents a comparison between the compliant over-running clutch and its traditional rigid-body counterpart. The comparisons are based on such factors as manufacturing time, assembly and part count, peak static torque, and weight. The respective strengths and weakness of the compliant clutch as compared with the rigid-body clutch are discussed.

Chapter 8 contains a brief discussion of microelectromechanical systems (MEMS) and a compliant ratchet and pawl clutch at the micro level. Finally, Chapter 9 contains the conclusions and recommendations of the research.

Introduction to Over-running Clutches

2.1 Introduction

An over-running clutch transmits torque from the driven input to the output driver in one direction and free wheels or overruns (does not transmit torque) in the other direction. According to Bickford, 1968, there are three basic uses for over-running clutches. First, they drive the load in only one direction while allowing it to coast in the other direction; second, they act as a backstopping device; and third, they can turn reciprocal motion into intermittent motion (indexing). Depending on the various applications, this class of clutches is capable of transmitting torques as small as a few inch pounds to over 700,000 foot pounds. Some possible applications in these three areas are discussed below.

2.1.1 One-way Operation

Over-running clutches may be used in any application where it is desired that the load be driven in one direction and allowed to coast or free-wheel in the opposite direction. A list of possible areas of application includes:

1. Unidirectional drives such as automotive differentials.
2. Speed compensation - for example, several motors with clutches used to feed material from a press. If the feed rate at the beginning of the line is faster than the feed rate at the end of the line, the motors at the beginning of the line will overrun to compensate for the lower speed at the end of the line.
3. Over-running applications such as automotive cooling fans that overrun when the motor stops to reduce belt breakage. Other automotive examples include starter motors, automatic transmissions, and farming equipment.
4. Applications where two prime movers are used to drive the same load such as a grinding machine where the grinding wheel shaft is connected to a low speed motor and a high speed motor. At high speeds, the low speed motor is allowed to overrun. Other areas for application where two prime movers are used include electrically powered refrigeration units and dry cleaning machines.

2.1.2 Backstopping

Over-running clutches may also be used as a backstopping device. In this application, they overrun in the direction of desired travel and prevent any motion in the opposite direction. The clutch acts as a stopping or counter rotation holding device. The primary application area is in the use of conveyor belts. As long as the machinery is functioning properly the clutch overruns. In the event that the power is interrupted and the machinery shuts down, the over-running clutch engages and will not allow the conveyor to counter rotate.

2.1.3 Indexing

Perhaps one of the most common applications of over-running clutches is indexing. The over-running clutch provides an intermittent stepping motion that has many uses that vary from light load applications to heavy load applications. As an indexing mechanism, over-running clutches are widely used as material feed mechanisms in shearing presses, punch presses, cut-off length control, automatic infeed and wire feeding. Their intermittent motion is also put to use in washing machine transmissions, dispensers, copying machines, check processors, collators, labeling and packaging machines, indexing tables, capsulating machines and candy machines.

For light load applications, the compliant clutch is an excellent alternative to its rigid-body counterpart. In many applications it can directly replace the rigid-body ratchet clutch and because of its low manufacturing cost, it may now be feasible to use this type of over-running clutch in applications where it was once not economically feasible to do so.

2.2 History of over-running clutches

Over-running clutches have been in use for several hundred years. One of the earliest drawings and conceptions of an over-running type clutch was drawn by Leonardo da Vinci some time during the late 1400's (1470-1500). Figure 2-1 shows da Vinci's version of a ratchet type clutch on a catapult. Burstall, 1963, documents the early use of ratchet and pawl type clutches in clocks during the fifteenth century.

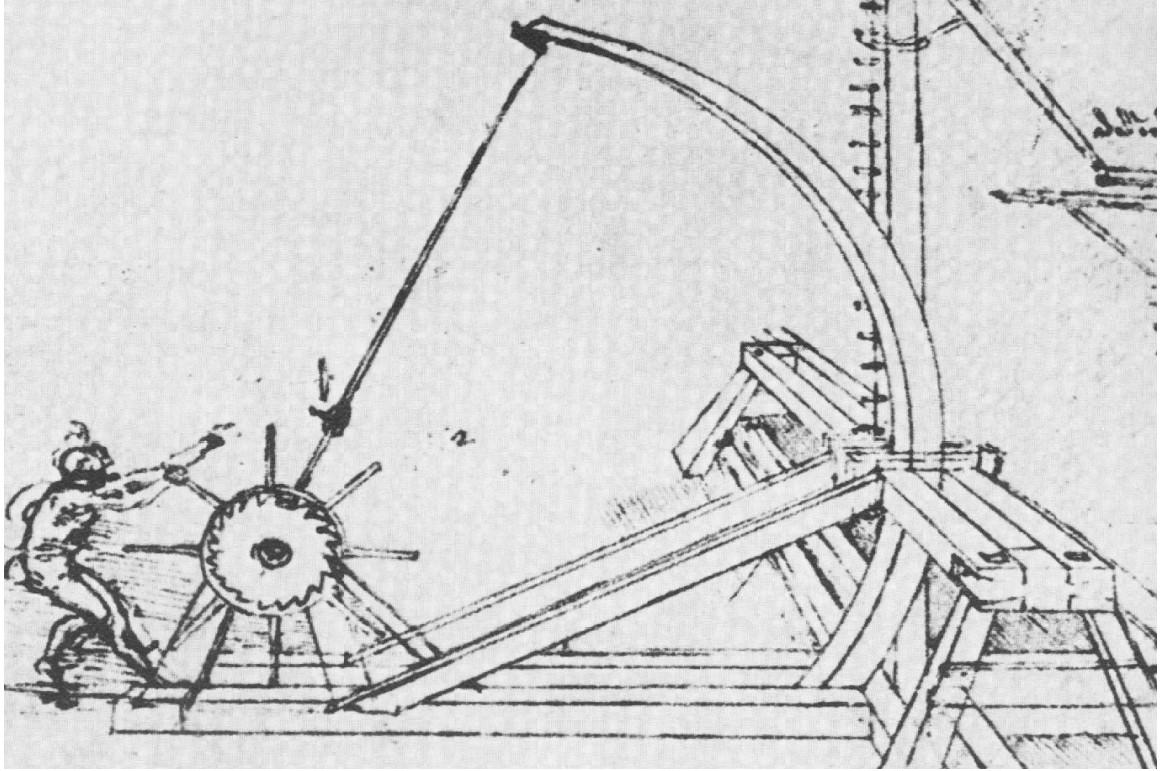


Figure 2-1 Leonardo da Vinci's sketch of a compliant catapult with a ratchet (Smith and Rees, 1978).

In 1729 Christopher Polheim made use of a ratcheting type clutch for indexing in his hand operated gear-cutting machine (Burstall, 1963).

With the advent of the Industrial Revolution, the inventions of the steam engine (eighteenth century) and the internal combustion engine (nineteenth century) provided mechanical power for many important technological advances (Forbes, 1963). Many of these new applications would require the use of over-running clutches in many different areas.

In the late 1870's, free-wheeling clutches began to appear on bicycles, which allowed bicyclists to coast without the pedals still turning. The clutch used by Schwinn, 1945, shown in Figure 2-2, incorporated rolling balls that wedge between the inner

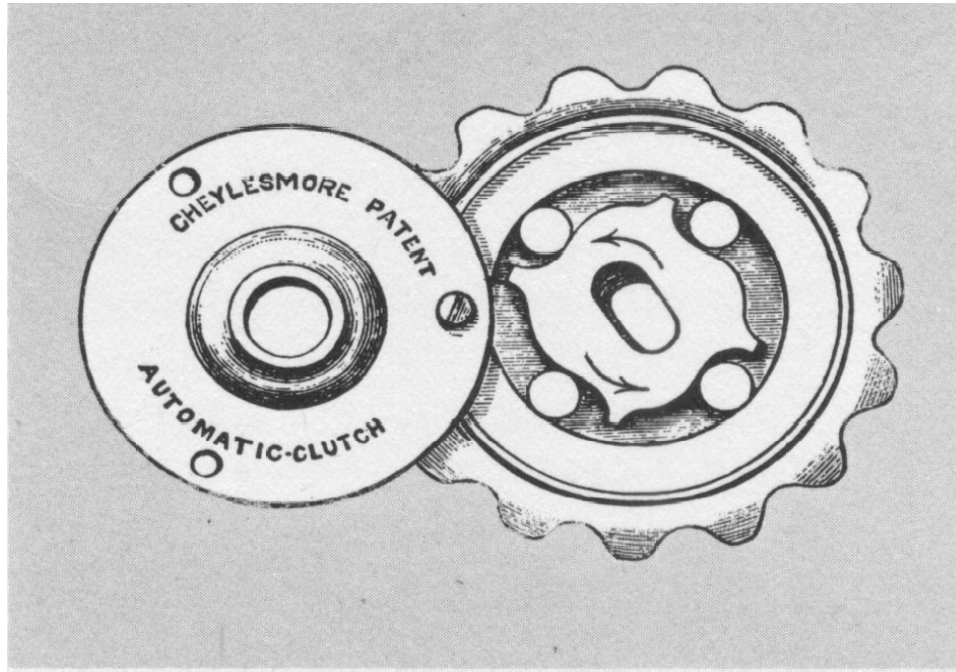


Figure 2-2 Schwinn 1870 free-wheeling roller clutch (Schwinn, 1945).

cammed surface and the outer ring to transmit torque in the driven direction, while over-running in the other direction. According to Schwinn, 1945, this device was the forerunner to the free-wheeling clutches used in early automobiles.

2.3 Types of over-running clutches

The four most common types of over-running clutches are the spring clutch, the roller clutch, the sprag clutch, and the ratchet and pawl clutch. A brief description of each clutch type is provided below.

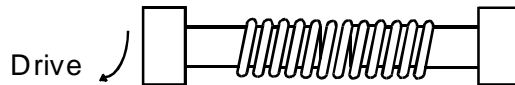


Figure 2-3 A wrapped spring clutch.

2.3.1 The Spring Clutch

The spring clutch consists of a helically wound spring wrapped around both the input driver and the output driven shafts, and is attached to the driver (Figure 2-3). This clutch type is a compliant mechanism. When the input driver rotates in one direction, the spring tightens and the friction increases, locking the two shafts together. When the input driver rotates in the other direction, the spring loosens and overruns with relatively small friction produced by the spring. Orthwein, 1986, provided equations for the torque that can be transmitted and the torque in the over-running direction. These equations are based on the first design of this type of clutch done by Wiebusch, 1939. Lowery and Mehrbrodt, 1976, developed equations for torque capacity and interference stresses.

Spring clutches have several advantages: very quick engagement, ability to be externally controlled, simple construction and few parts. Nevertheless, they are not well suited to high speed applications, and often wear quickly.

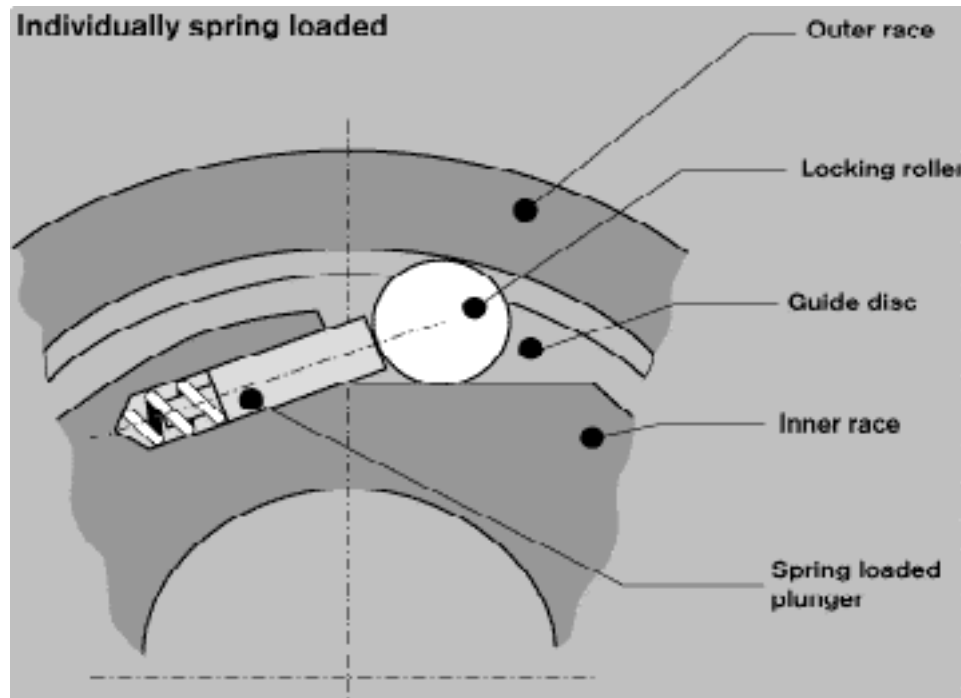


Figure 2-4 Typical roller clutch diagram (Stieber [http:// www.riv.org/stieber.htm](http://www.riv.org/stieber.htm)).

2.3.2 The Roller Clutch

Several configurations exist for roller type clutches. All of them operate with the same basic principles. Balls or rollers run between an outer and an inner race. One of the races is profiled so that the balls or rollers rotate freely in one direction and wedge or lock in the other direction to transmit torque. The free-wheeling Schwinn clutch, shown in Figure 2-2 is a good example of a roller clutch. Modern roller clutches use a spring to keep the roller or ball in contact with the inner and outer race. A basic diagram of a roller clutch is provided in Figure 2-4. Orthwein, 1986, provided equations for the torque transferred

and for analysis of the contact stresses in the rollers. This analysis is important because the torque transmitted by the clutch is limited by the amount of contact stress that can be withstood by the rollers. South and Mancuso, 1994, gave a mathematical model for determining lockup angle and the normal force required to drive the load.

Roller clutches have the advantages of not transmitting torque until the input driver is rotating faster than the output, and they are fairly inexpensive. Notwithstanding, these clutches tend to have some friction and wear issues.

2.3.3 The Sprag Clutch

One of the more frequently used clutches in applications requiring over-running is the sprag clutch. Instead of using rollers between the inner and outer race, sprag clutches incorporate a series of sprags placed around the entire inner race. The sprags are designed to be thinner than rollers or balls so that more of them can fit into the allotted space, thus increasing the torque that can be transmitted. The sprags also have an increased radius of curvature along the line of contact with the inner and outer race. All of the sprags are canted in one direction (gripping angle) to offset the contacting points. This allows for the increased radius of curvature to be used and also provides the free wheeling and wedging action of the clutch. All of the sprags are held in place by a sprag retainer, and an energizing spring keeps the sprags in contact with the inner and outer races so that the sprags are already in the correct position when the clutch is engaged. A sprag clutch is shown in Figure 2-5.

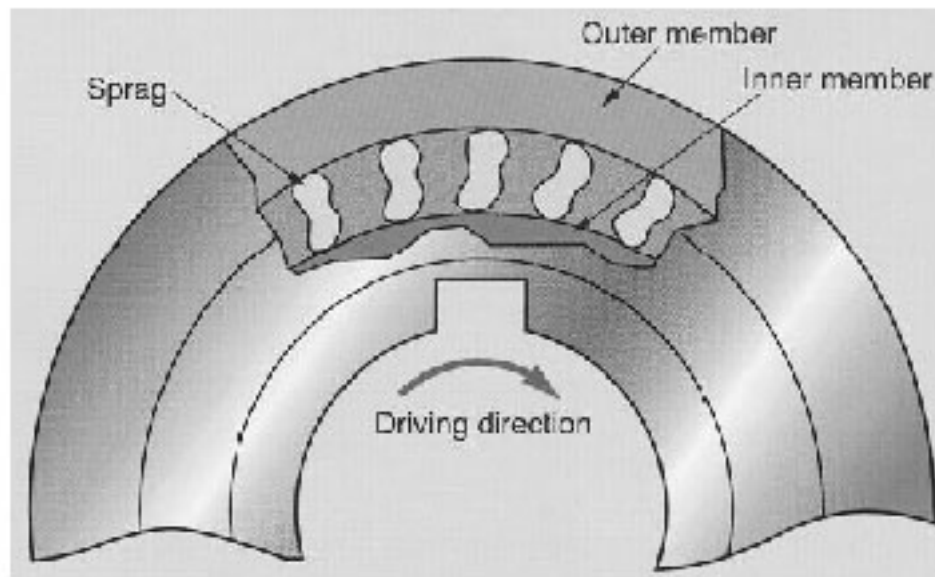


Figure 2-5 Typical sprag clutch diagram (Hilliard Corporation <http://www.hilliardcorp.com/images/sprag.jpg>).

Orthwein, 1986, presented equations for determining the gripping angle, and the minimum radii of curvature for the inner and outer sprag profiles. Xu and Lowen, 1993, introduced a complete mathematical model for a sprag clutch. Their model provided for the inertias of the springs and the output race and the Hertzian contact stresses between the sprags and the races. They also presented a new non-linear method for determining the damping force.

Sprag clutches have the advantage of being able to transmit large torques for a small clutch. According to Daniels, 1967, the load carrying capacity is greater than that of any other over-running clutch of the same size dimensions. Friction is also not so much of a concern with sprag clutches, however, they do have a higher cost and increased part count (the part count is higher than any other type of over-running device because of the number of sprags incorporated).

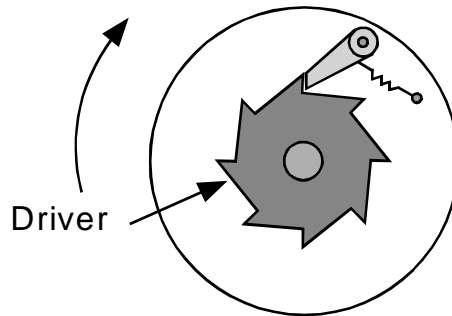


Figure 2-6 A ratchet and pawl clutch.

2.3.4 The Ratchet and Pawl Clutch

The ratchet and pawl clutch is one of the simplest over-running designs. The simplest of these designs uses a single pawl and ratchet. The pawl can be attached either to the outer hub or the inner hub. The pawl is spring loaded, allowing it to pivot out of the way of the ratchet when it free wheels, but forcing it into engagement in the torque transmitting direction. An example is given in Figure 2-6.

Ratchet and pawl clutches can also be designed with multiple pawls, where only one pawl at a time actuates or where more than one pawl engages to transmit the torque.

Chironis and Rossner, 1991, presented an analysis for a ratchet and pawl clutch. Their model provides for the layout of the pawls and gives equations for the self-engagement of the pawls so that the spring force is not completely relied upon to engage the clutch.

The advantages of the ratchet and pawl clutch are its simplicity and low cost. The weaknesses of the ratchet and pawl clutch are the inherent noise that the pawls make when free wheeling, and the possibility of requiring a rotation before engagement due to the location of the pawl and the pitch of the ratchet gear (backlash).

3.1 Introduction

Compliant mechanisms, by definition, are mechanisms that gain some or all of their motion from the deflection of their members. This makes them very different from traditional rigid-body mechanisms which have rigid links connected by kinematic pairs such as pin joints, sliding joints, and cams. Compliant mechanisms can also be classified as fully compliant, or partially compliant. Figure 3-1(a) shows an example of a traditional rigid-body parallel guiding mechanism and Figure 3-1(b) shows a partially compliant parallel mechanism consisting of two compliant links and two kinematic pairs (Derderian et al., 1996). Figure 3-2 is an example of a fully compliant parallel guiding mechanism.

Compliant mechanisms offer several advantages, one of the most important of these is that they have a reduced overall part count compared to their rigid-body counterparts. For example, the rigid-body version of the parallel guiding mechanism (Figure 3-1(a)), requires at least eight parts for assembly (links and pins), and the fully compliant

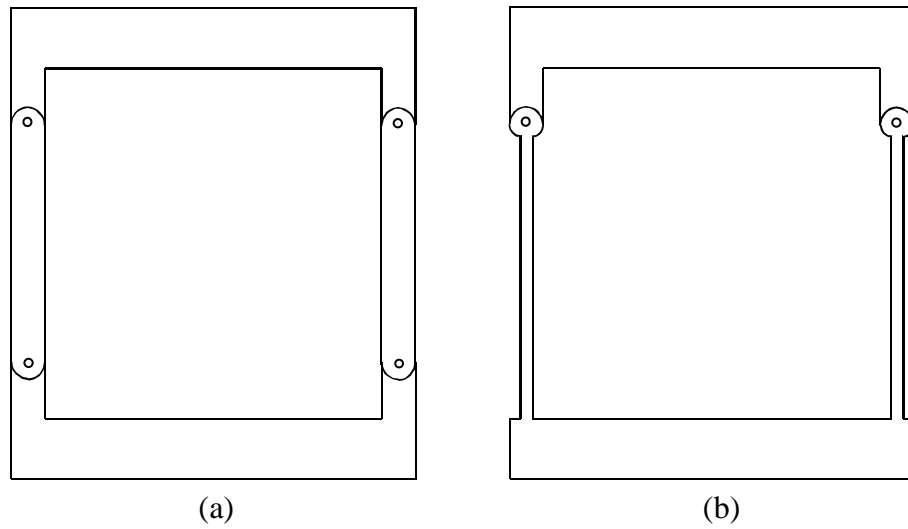


Figure 3-1 (a) A rigid-body parallel guiding mechanism and (b) a partially compliant parallel guiding mechanism.

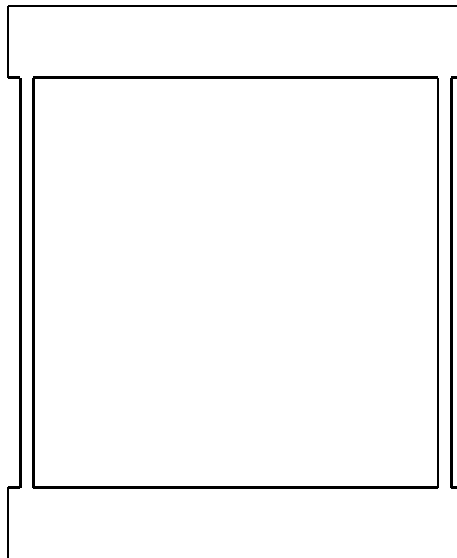


Figure 3-2 A fully compliant parallel guiding mechanism.

parallel mechanism (Figure 3-2) can be manufactured from a single piece of material while performing the same function. This advantage makes compliant mechanisms ideal

for applications in microelectromechanical systems (Ananthasuresh et al., 1992; Ananthasuresh et al., 1993; Ananthasuresh, 1994; Kota et al., 1994; Ananthasuresh et al., 1996; Derderian, 1996; Larsen et al., 1996; Jensen et al., 1997). In addition to lowering the part count, the use of compliance may also produce a reduction in overall weight. According to Sevak and McLarnan, 1974, other advantages include minimum part wear, lower noise, higher precision and increased reliability. Compliant mechanisms also have less backlash due to a decrease in the number of kinematic pairs, and they require less lubrication. They are well suited for applications requiring operation in harsh environments.

Although compliant mechanisms do offer many advantages over traditional rigid-body mechanisms, they do come with their own challenges, the greatest of which is the difficulty in designing and analyzing them. The design is difficult because compliant mechanisms store energy in their flexible members, and the flexible members often go through such large deflections that the linear small-deflection equations used for analyzing beam deflections are not accurate. These geometric nonlinearities require nonlinear analysis methods, such as, the pseudo-rigid-body model method for designing compliant mechanisms that will be presented in Chapter 4. Other disadvantages (Howell and Midha, 1997) include stress relaxation or creep, limitations in motion (a compliant link attached to ground cannot function completely as a fully rotational pin joint), and increased importance of fatigue considerations because the compliant segments are often subjected to alternating loads.

An understanding of the advantages and disadvantages of compliant mechanisms is helpful in determining those applications best suited for the use of compliance.

3.2 Literature Review

The first analysis of deflecting members was done by Bernoulli and Euler, yielding the classic beam equation which states that the bending moment is proportional to the curvature

$$M = EI \frac{d\theta}{ds} = EI \frac{\frac{d^2y}{dx^2}}{\left(1 + \left(\frac{dy}{dx}\right)^2\right)^{\frac{3}{2}}}. \quad (3.1)$$

For the assumption that the deflections are small, (the square of the slope dy/dx is negligible) this equation reduces to

$$M = EI \frac{d^2y}{dx^2} \quad (3.2)$$

However, in the realm of large deflection analysis, this assumption is no longer valid. The square of the slope, (dy/dx) in the Bernoulli-Euler equation can no longer be assumed to be negligible because the slope is increasing as the deflection increases. Finding an analysis technique to model large deflections has been the subject of research for many years. Bisshopp and Drucker, 1945, were the first to find a solution to determine the large deflection of cantilever beams. They used complete and incomplete elliptic integrals to find a closed-form solution of a second order non-linear differential equation. Frisch-Fay, 1962, also addressed this problem. Elliptic integrals have been used to design compliant mechanisms (Burns, 1964; Burns and Crossley, 1966; Shoup and McLarnan, 1971; Shoup, 1972; Mat-

tiasson, 1981; Howell and Leonard, 1997). Although the use of elliptic integrals provides closed-form solutions, the method can only be used to solve problems involving simple geometries and loadings. This makes the application of this method to the design of entire compliant mechanisms quite difficult. The method also assumes that bending does not alter the length of the beam and that the material is inextensible.

Further research has focused on using numerical methods to find approximations to the actual solutions of force-displacement characteristics of flexible members.

Boronkay and Mei, 1970, used the finite element method to analyze a flexible link mechanism (a mechanical adder). Sevak and McLarnan, 1974, used finite element analysis and the variable metric method of optimization developed by Fletcher and Powell to do non-linear large deflection analysis and synthesis of flexible link mechanisms. Gandhi and Thompson, 1980, incorporated a mixed variational principle with finite element to determine the stresses and deflections of a general planar linkage mechanism, and to study the vibrations in the flexible members. Their method allows for arbitrary variations in stress, strain, velocity and displacement. This variational method yields the governing differential equations and the proper boundary conditions for the finite element model. Finite element analysis is still commonly used in the design of compliant mechanisms. Nevertheless, it does have some challenges, sometimes the nonlinear solution does not converge and it can be computationally expensive and time consuming. Probably the major challenge is that it is assumed that the geometry is already known, which is not the case in early stages of compliant mechanism synthesis.

Other numerical methods exist for the analysis of non-linear large deflections that aid in the design of compliant mechanisms. Miller, 1980, proposed a shooting method

along with Newton-type iteration to approximate the solutions of a continuously flexible member with arbitrary initial shape and loading. The member is modeled by a set of elements all connected together at nodal points and numbered consecutively. Loads are applied at the nodal points and temperature changes, if any, are applied to each element. The equations for equilibrium are then solved for each node, beginning at the first and proceeding along the chain. The Newton-type iteration is used to determine any of the unknown values that are not prescribed. Like other numerical methods, Miller's method is not guaranteed to converge and may require significant computational time. Coulter and Miller, 1988, extended this method to provide for non-linear material behavior.

Lewis and Monasa, 1981 used a fourth-order Runge-Kutta method to solve the second order non-linear differential equation derived from the Bernoulli-Euler bending moment curvature equation and the Ludwick stress strain equation. The solution to this equation provides the vertical and horizontal deflections and rotations along the central axis. Like elliptic integral methods, this technique provides solutions for simple geometries and loadings.

The implementation of a graphical based "user-driven" Newton-Raphson technique by Hill and Midha, 1990, provided another tool for use in analyzing large deflections and designing compliant mechanisms. The method uses beam elements with six degrees of freedom in a chain calculation. The chain calculation combines the displacements of each element (due to the applied loads) to find the total deflection. The disadvantages of the method are that it does not provide the user with any initial load estimates, only the results of the loading, and the process may diverge.

Another development of a chain calculation method was proposed by Midha et al., 1992. This method uses a load incrementing technique that estimates the moment arms with increased accuracy, thus increasing the overall accuracy of the approximation, and a transformation matrix that relates the global elastic displacements of an element with its local displacements. This chain algorithm is used in conjunction with a shooting method developed by Her et al., 1992, that uses Newton-Raphson and optimization techniques to reduce the closure errors for the displacement boundary conditions and to improve the design to meet the desired objective.

Other methods exist for designing compliant mechanisms that don't include the evaluation or consideration of large non-linear deflections. For example, structural optimization and homogenization theory has been proposed to design compliant mechanisms with a beginning set of loading and motion requirements (Ananthasuresh et al., 1992; Kota et al., 1994; Ananthasuresh, 1994; Ananthasuresh and Kota, 1995; Ananthasuresh et al., 1996; Ananthasuresh and Kota, 1996). Frecker et al. (1995, 1996), used multi-criteria optimization to satisfy the kinematic and structural requirements. This method works for mechanisms that are required not only to be flexible to satisfy motion requirements, but also stiff to support external loadings. A penalty function was later added to this method to increase convergence (Frecker et al., 1997). Parkinson et al., 1997, proposed a method to design compliant mechanisms that incorporates a parametric optimization and finite element analysis technique.

The methods presented above require extensive effort to set up the models and call for sizeable computation time to arrive at the solutions. A pseudo-rigid-body model was introduced that not only aids in constructing the initial model for other methods such as

those described above, but also can be used by itself to fulfill the given design requirements for a mechanism (Howell, 1991; Howell and Midha, 1995). The pseudo-rigid-body model allows for a compliant mechanism to be modeled as a pseudo-rigid-body mechanism. This new modeling technique is able to use the extensive knowledge already available about rigid-body kinematics to design compliant mechanisms. Howell and Midha, 1995, proposed the model to approximate the non-linear deflections of end-loaded cantilever beams. The path coordinates were parameterized in terms of a pseudo-rigid-body angle. The approximations were found to be accurate to within 0.5 percent of the closed form elliptic integral solutions. Later, a stiffness coefficient was added to the model to provide simple force-deflection characteristic approximations (Howell et al., 1996). A standard nomenclature was proposed by Midha et al., 1994, to aid in research being done across several disciplines. The method has since been expanded in conjunction with Burmester theory to design compliant mechanisms for four and five precision point synthesis (Mettlach and Midha, 1996). This new modeling technique provides for simplified modeling and design of compliant mechanisms and is the modeling technique used in this research.

3.3 The Pseudo-Rigid-Body Model

As stated above, the pseudo-rigid-body model is an efficient method to approximate the large deflections in compliant members. The model uses rigid links and torsional springs to represent force-deflection characteristics of compliant systems. The rigid-link systems can be analyzed using traditional mechanism theory. Thus, the model connects traditional mechanism theory with compliant mechanism theory.

3.3.1 The Pseudo-rigid-body Model for Cantilever Beams

Howell and Midha, 1995, developed a model for an arbitrarily end-loaded cantilever beam. As the deflection of the beam increases, the classical beam moment equation given in Equation (3.2) is no longer valid and the exact differential equation provided in Equation (3.1) must be used. This model builds on the assumption by Burns, 1964, and Burns and Crossley, 1968, that the deflection path of a cantilever beam with arbitrary end forces is very similar to an arc centered at one-sixth the length of the beam from the fixed end and traversing a path of five-sixths radius. Howell modeled this deflection using two rigid links joined by a pivot. Also, a non-linear spring was placed at the pivot to model the deflection resistance. The pivot is called the “characteristic pivot” and the link is referred to as a “pseudo-rigid-body link.” The characteristic pivot is placed at a distance (γl) from the free end of the beam. The parameter γ is defined as the “characteristic radius factor,” and the product (γl) is the “characteristic radius,” or the radius of the path that the pseudo-rigid-body link traverses as it deflects. The angle through which the pseudo-rigid-body link travels is called the “pseudo-rigid-body angle” (Θ) . The x and y coordinates of the deflected tip are represented by a and b . The variable n represents the ratio of the axial load to the transverse load. A deflected cantilever beam and its corresponding pseudo-rigid-body model are provided in Figure 3-3. As the deflection of the beam increases, at some point the error in the approximation begins to increase; so in choosing the value for γ an acceptable value of error must be specified. A maximum error of 0.5% was chosen, and optimization was used to find the best value for γ that would yield the largest pseudo-

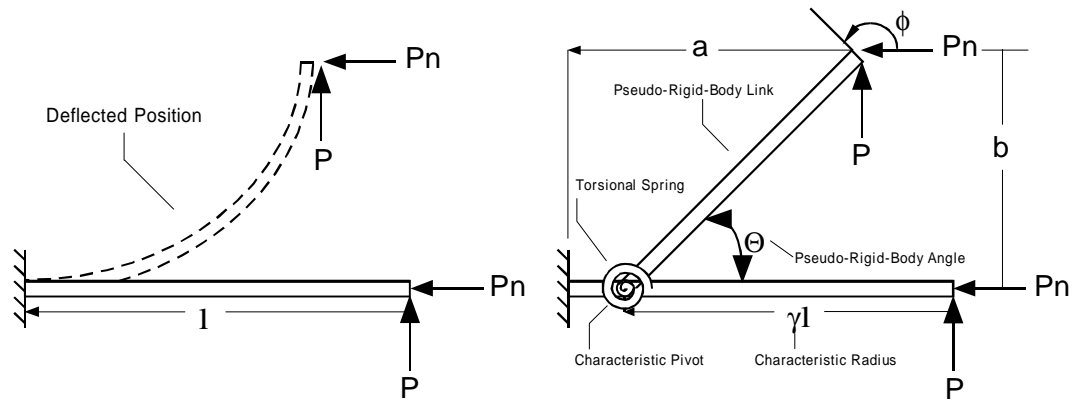


Figure 3-3 A cantilever beam in its initial and deflected position and its corresponding pseudo-rigid-body model.

rigid-body angle. It was determined that for $n = 0$ (vertical end load only), the optimal value of $\gamma = 0.8517$. This value is within the 0.5% error and produces an angular deflection of 77° . This represents a vertical deflection of almost 80% of the beam length. As n increases the value of γ changes also. Values for γ given differing values for n can be determined from the following equations (Howell and Midha, 1995):

$$\gamma = 0.841655 - 0.0067807n + 0.000438n^2; 0.5 < n < 10.0 \quad (3.3)$$

$$\gamma = 0.852144 - 0.0182867n; -1.8316 < n < 0.5 \quad (3.4)$$

$$\gamma = 0.912364 + 0.0145928n; -5.0 < n < -1.8316 \quad (3.5)$$

An average γ value of 0.85 can be used for rough calculations.

The end coordinates of the deflected beam in the pseudo-rigid-body model may be found from the following non-dimensional equations using γ and the pseudo-rigid-body angle:

$$\frac{a}{l} = 1 - \gamma(1 - \cos \Theta) \quad (3.6)$$

$$\frac{b}{l} = \gamma \sin \Theta \quad (3.7)$$

Howell and Midha, 1995, also determined the relationship between the pseudo-rigid-body angle, Θ approximation and the actual angular deflection, θ_0 . The relationship between the two is almost linear and θ_0 can be approximated by:

$$\theta_0 = c_\theta \Theta \quad (3.8)$$

where the constant c_θ is called the “parametric angle coefficient.” As the loading changes, the value for c_θ also changes. Table 3-1 provides values for c_θ for differing values of n .

The total force acting on the end of the beam can be expressed as:

$$F = \sqrt{P^2 + (nP)^2} = \eta P \quad (3.9)$$

with

$$\eta = \sqrt{1 + n^2} \quad (3.10)$$

The pseudo-rigid-body model with applied component forces is shown in Figure 3-4. The transverse component of the force, F_t , can be expressed in terms of the nondimensionalized transverse load index, $(\alpha^2)_t$, as

$$(\alpha^2)_t = \frac{F_t l^2}{EI} \quad (3.11)$$

where

$$F_t = F \sin(\phi - \Theta) = \eta P \sin(\phi - \Theta) \quad (3.12)$$

with ϕ being the angle of the applied load as shown in Figure 3-3.

Norton, 1991, and Howell et al., 1996, found that in plotting the nondimensionalized transverse load index, $(\alpha^2)_t$, versus the pseudo-rigid-body angle, Θ , a nearly linear

Table 3-1: Values for c_θ for various angle of force (Howell and Midha, 1997).

n	c_θ
0.0	1.2385
0.5	1.2430
1.0	1.2467
1.5	1.2492
2.0	1.2511
3.0	1.2534
4.0	1.2584
5.0	1.2557
7.5	1.2570
10.0	1.2578
-0.5	1.2348
-1.0	1.2323
-1.5	1.2322
-2.0	1.2293
-3.0	1.2119
-4.0	1.1971
-5.0	1.1788

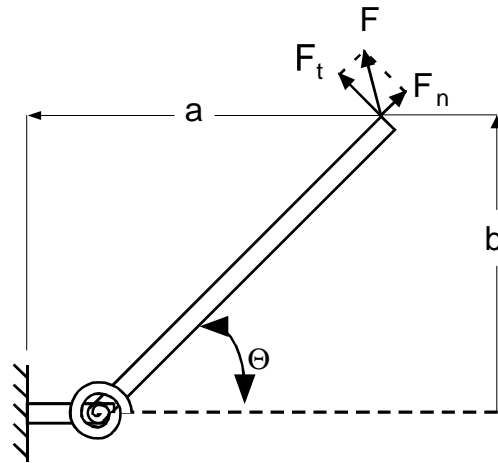


Figure 3-4 The pseudo-rigid-body model of a cantilever beam with applied component forces.

relationship exists. Using this idea, the force-deflection relationship can be presented in the following equation:

$$(\alpha^2)_t = K_{\Theta} \Theta \quad (3.13)$$

where K_{Θ} is termed the “stiffness coefficient.” Therefore, the stiffness of the torsional spring in the pseudo-rigid-body model is constant for a constant value of n . Nevertheless, the force-deflection relationship may not be accurate over the total model. Values for K_{Θ} vary for different values of n and may be derived for varying load conditions from the following:

$$K_{\Theta} = 3.024112 + 0.121290n + 0.003169n^2 \quad -5.0 < n < -2.5 \quad (3.14)$$

$$K_{\Theta} = 1.067647 - 2.616021n - 3.738166n^2 - 2.649437n^3 - 0.891906n^4 - 0.113063n^5 \quad 2.5 < n < -1 \quad (3.15)$$

$$K_{\Theta} = 2.654855 - 0.509896 \times 10^{-1}n + 0.126749 \times 10^{-1}n^2 - 0.142039 \times 10^{-2}n^3 - 0.584525 \times 10^{-4}n^4 \quad -1 < n < 10 \quad (3.16)$$

A value of $K_{\Theta} = 2.65$ or $K_{\Theta} = \pi\gamma$ may be used for a quick approximation.

The torque, T , at the characteristic pivot on the model, is given as the product of the torsional spring constant, K , and the pseudo-rigid-body angle, Θ :

$$T = K\Theta \quad (3.17)$$

This torque may also be written as

$$T = F_t\gamma l \quad (3.18)$$

Combining Equation (3.17) and Equation (3.18) and solving for F_t results in

$$F_t = \frac{K\Theta}{\gamma l} \quad (3.19)$$

with the value of the torsional spring constant, K as

$$K = \gamma K_{\Theta} \frac{EI}{l} \quad (3.20)$$

3.3.2 The pseudo-rigid-body model for initially curved cantilever beams

While the above model is suitable for end-loaded cantilever beams, a different model is required for an initially curved cantilever beam. Howell and Midha, 1996, presented a method for modeling initially curved end-loaded cantilever beams. Figure 3-5 shows an initially curved end-loaded cantilever beam with radius of curvature, R_i . The

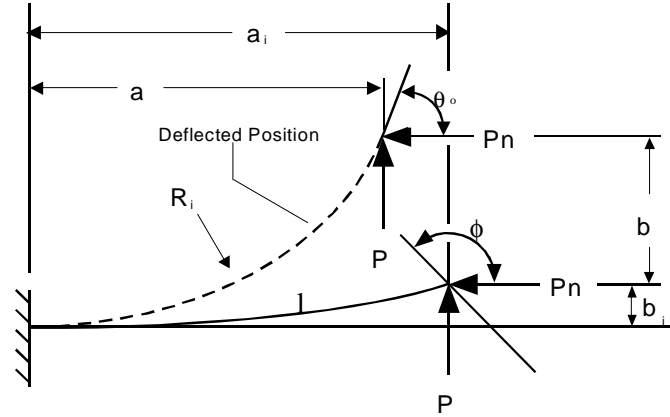


Figure 3-5 An initially curved cantilever beam in its initial and deflected positions.

variables P and P_n , are the vertical and horizontal components of the end loads, and a and b represent the x and y coordinates of the beam end. The parameter κ_0 relates the initial radius of curvature to the beam length and is defined as

$$\kappa_0 = \frac{l}{R_i} \quad (3.21)$$

The pseudo-rigid-body model for the curved beam is provided in Figure 3-6. The characteristic radius factor, γl , is measured along the beam as if it were initially straight. The length of the pseudo-rigid-body link, ρl , is a function of γ and the beam curvature. The pseudo-rigid-body angle, Θ_i , due to the initial curvature of the beam may be expressed by

$$\Theta_i = \text{atan}\left(\frac{b_i}{a_i - l(1 - \gamma)}\right) \quad (3.22)$$

where a_i and b_i are the initial undeflected x and y coordinates at the free end of the segment. The value for ρ , the characteristic radius factor is given as

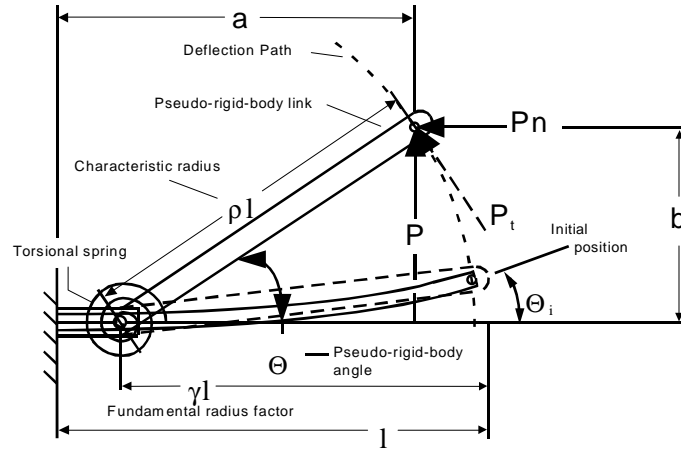


Figure 3-6 The pseudo-rigid-body model of an initially curved end-loaded cantilever beam.

$$\rho = \left[\left(\frac{a_i}{l} - (1 - \gamma) \right)^2 + \left(\frac{b_i}{l} \right)^2 \right]^{\frac{1}{2}} \quad (3.23)$$

with a_i and b_i being determined by the following,

$$\frac{a_i}{l} = \frac{1}{\kappa_o} \sin \kappa_o \quad (3.24)$$

and

$$\frac{b_i}{l} = \frac{1}{\kappa_o} (1 - \cos \kappa_o) \quad (3.25)$$

The coordinates of the deflected end of the segment, a and b , are approximated by the pseudo-rigid-body model as

$$\frac{a}{l} = 1 - \gamma + \rho \cos \Theta \quad (3.26)$$

and

$$\frac{b}{l} = \rho \sin \Theta \quad (3.27)$$

The stiffness coefficient for the initially curved segment can be expressed in terms of the nondimensionalized transverse load index, $(\alpha^2)_t$, and the pseudo-rigid-body angles, Θ and Θ_i as

$$\alpha_t^2 = K_\Theta (\Theta - \Theta_i) \quad (3.28)$$

The torque at the characteristic pivot may be written

$$T = \rho l P_t \quad (3.29)$$

where P_t is the component of the force tangential to the deflection path. The torque may alternately be expressed using the torsional spring constant, K to give

$$T = K(\Theta - \Theta_i) \quad (3.30)$$

where

$$K = \rho K_\Theta \frac{EI}{l} \quad (3.31)$$

Howell and Midha, 1996, also provided recommendations for values for γ , ρ , and K_Θ for differing values of κ_0 . These values are provided in Table . The actual angle of deflection of the free end of the segment may be approximated by the model as

$$\theta_0 = c_\Theta (\Theta - \Theta_i) + \theta_{0i} \quad (3.32)$$

where c_θ is given in Table 3-1 and $\theta_{0i} = l/R_i$.

3.3.3 The pseudo-rigid-body model for small-length flexural pivots

Another model type is the pseudo-rigid-body model for small-length flexural pivots. A small-length flexural pivot consists of a rigid segment joined to a short flexible segment that acts as a pin joint. For this to work, the length of the rigid segment is required to be significantly greater than the length of the flexible segment. Howell and Midha, 1994, presented a method for modeling small-length flexural pivots. Figure 3-7 shows a small-length flexural pivot in its original and deflected position, and the appropriate pseudo-rigid-body model.

Table 3-2: Values for γ , ρ , and K_Θ for differing κ_0

κ_0	γ	ρ	K_Θ
0.00	0.85	0.850	2.65
0.10	0.84	0.840	2.64
0.25	0.83	0.829	2.56
0.50	0.81	0.807	2.52
1.00	0.81	0.797	2.60
1.50	0.80	0.775	2.80
2.00	0.79	0.749	2.99

$$K = \frac{EI}{l} \quad (3.35)$$

where E and I are the values for the small-length segment.

Pseudo-rigid-body models have also been developed for other loadings and configurations such as fixed-guided flexible segments (Howell et al., 1996), and functionally binary, pinned-pinned segments (Edwards, 1996).

The different pseudo-rigid-body models can be combined together to form more complex mechanisms such as the fully compliant parallel guiding mechanism in Figure 3-2. The mechanism consists of two fixed-guided flexible segments joined by rigid links. It is this ability to easily incorporate these pseudo-rigid-body segments in mechanism design that makes the pseudo-rigid-body model such a powerful design tool.

The pseudo-rigid body models for the end-loaded cantilever beam and the small-length flexural pivot are used to design different compliant segments in the ratchet and pawl type clutches that are presented. The pseudo-rigid body model for initially curved cantilever beams is provided because of its possible application in the design process.

Clutch Type Comparison and Alternative Ratchet and Pawl Designs

4.1 Introduction

In order to determine which type of over-running clutch is best suited to benefit from the use of compliance, it is important to understand the factors or judging criteria that make mechanisms, in general, good candidates for compliance. Only those factors that apply to over-running clutches are discussed and used to evaluate the different types of over-running clutches.

4.1.1 Revolute Joints

Mechanisms containing rigid-body revolute joints are good candidates for the use of compliance. These joints can sometimes be replaced by compliant segments that provide the same type of motion. The replacement of revolute joints by compliant segments also reduces backlash in the mechanism and can increase precision.

4.1.2 Possible Part Count Reduction

One of the advantages to using compliant mechanism theory in design is the possible reduction in part count. In replacement applications, it is important for the mechanism to contain a significant number of parts. The higher the number of parts, the greater the opportunity for the use of compliance to have a large impact on part reduction. A reduction in parts often leads to a reduction in cost and a reduction in the time required for manufacturing and assembly.

4.1.3 Springs in the System

If the mechanism to be replaced contains springs, they may be replaced by compliant segments that serve to accomplish the same function. The compliant segments are able to store energy and thus behave like a spring in some applications.

4.1.4 Joint Revolution Requirements

The amount of revolution required in the revolute joints has a large effect on whether or not compliance may be used. If the joint requires a full 360 degree rotation, then a compliant segment is not an option. However, if the required rotation is small, compliant segments can be considered as a possible alternative.

4.1.5 Possible Reduction in Weight

If the introduction of compliance produces an overall reduction in the weight of the mechanism then cost may be reduced by requiring less material. The lower weight may also be considered a benefit in those applications where weight is a design constraint.

4.1.6 Clutch Engagement

Over-running clutches use different methods for engagement. Clutch types that engage by two parts that interlock are more suitable for the use of compliance than are clutch types that engage by friction. Some friction type over-running clutches require a full rotation of the friction device such as a ball or a spring, this makes the use of compliance in these applications difficult or even impossible.

4.2 Over-running Clutch Comparison

With an understanding of the criteria that make a mechanism a good candidate for the use of compliance, each type of clutch is now examined and evaluated on how well it meets these criteria. From this comparison the most promising clutch is chosen for further investigation.

The results of the clutch comparisons are presented in Table 4-1 Positive correlations are shown in the large bold font. The ratchet and pawl clutch type shows a positive correlation in all six areas indicating that it is the most promising clutch type for the use of compliance.

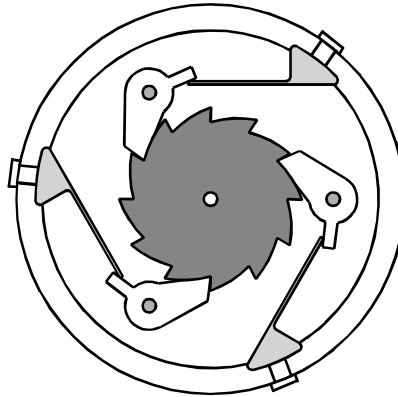


Figure 4-1 A rigid-body ratchet and pawl clutch with three pawls, pin joints, and leaf springs.

The traditional ratchet and pawl clutch shown in Figure 4-1 has the pawls rotating about pin joints. At a minimum, this type of clutch has a part count of 18 including only pins, pawls and springs (for a three pawl clutch). The clutch contains one spring for each pawl to keep the pawl in contact with the ratchet. For this clutch, the pawls are required to rotate only a small amount to clear the teeth so no full revolutions are required for the pin joints. A reduction in overall weight is also achievable if the springs and pin assemblies can be entirely removed.

Table 4-1: Over-running clutch type comparison

Clutch Type	Revolute Joints	Possible Part Count Reduction	Springs in the System	Joint Revolution Requirements	Possible Reduction in Weight	Clutch Engagement
Sprag	YES	YES	YES	NO	YES	FRICTION
Spring	NO	NO	YES	NO	NO	FRICTION
Roller or Ball	NO	YES	YES	YES	YES	FRICTION
Ratchet and Pawl	YES	YES	YES	NO	YES	INTERLOCK

It is interesting to note that the sprag type clutch has a positive correlation in five of the six areas. This may indicate that compliance might also be used to design clutches of this type as an area for further research.

4.3 Ratchet and Pawl Clutch Designs

The ratchet and pawl type of over-running clutch was shown to be the most promising candidate for the use of compliance. Recall that for a ratchet and pawl clutch, the pawl is forced into engagement with the ratchet teeth by a spring force, and in the free-wheeling direction the pawl deflects away from the ratchet teeth. The loading of the pawls can be accomplished in three different ways: loading the pawls in tension, loading the pawls in bending, and loading the pawls in compression. Designs involving the three means of loading the pawls are explored. In order to determine which of these designs is the best, all of the designs are rated by the ratio of output torque to free-wheeling torque with the best clutch design being the one with the highest rating.

Certain design parameters are kept constant among all the different designs in order to provide an unbiased comparison. First, all of the clutches incorporate only three pawls in their design. Second, the maximum normal force that the pawls may exert on the ratchet was set at 0.16 lb. Third, the maximum outer diameter for the hub was set at 4.0 in. For the comparison, all of the clutches were constructed using the same mill and material (0.25 in. polypropylene). Polypropylene was chosen because of its material properties (a high ratio of Young's modulus to strength) which make it excellent for use in compliant mechanism design.

The torques, output and free-wheeling, were measured using a hand-held digital strain gage and a reaction torque sensor. Peak static torque for the polypropylene clutch was measured by attaching a reaction torque sensor and a handheld strain gage indicator to a ratchet wrench and applying a torque until the clutch failed. The handheld strain gage indicator provides a digital read-out of the peak torque measured. Free-wheeling torque was measured using the same device with torque being applied in the over-running direction. The hubs of the clutches were fixed so that they could not be a source of failure. It is desired that the clutch fail in the pawls or the ratchet.

4.4 Bending Load Designs

The bending load designs are those clutches that support the output torque loading through bending of the pawls. Two different designs are presented and discussed. Their over-running and static torques were measured to obtain the comparison ratio of free-wheeling torque to static torque.

4.4.1 Bending Clutch Design 1

Figure 4-2 shows the first bending loaded pawl design. The pawls are slender cantilever beams that deflect easily away from the hub teeth in the free-wheeling direction. In the torque output direction, the cantilevers are forced against the hub teeth until the applied torque is such that the beams yield and fold over. The PRBM (pseudo-rigid-body model) used in the design is a simple cantilever beam. Figure 4-3 shows the PRBM superimposed on the cantilever beam. With the given design constraints, the parameters

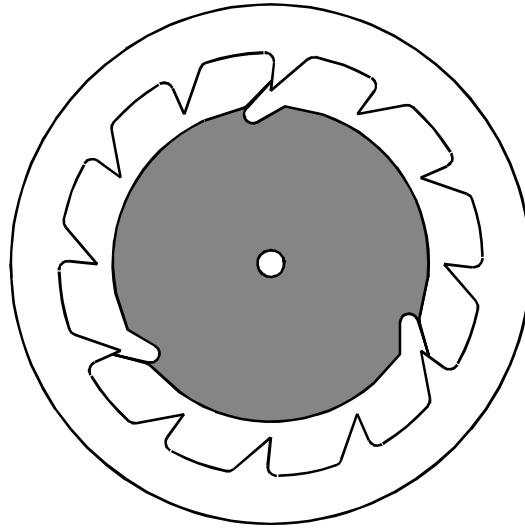


Figure 4-2 A compliant ratchet and pawl clutch. The pawls are loaded in bending in the torque output direction.

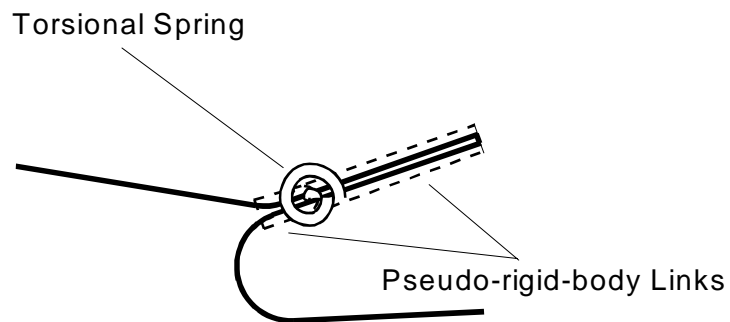


Figure 4-3 The pseudo-rigid-body model of the cantilever beam.

required to design the beam are the amount of deflection required for the beam to clear the hub tooth, the length of the cantilever beam, and the thickness of the cantilever beam. For this design, the length of the beam, l , and the deflection of the beam, b , were chosen to be

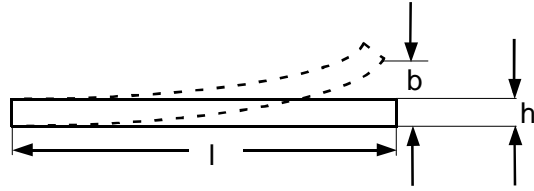


Figure 4-4 The cantilever beam with dimensional parameters.

0.18 in. and 0.06 in. respectively, and the thickness, h , is left to be determined. Figure 4-4 show the beam with its dimensional parameters. The beam is loaded with a vertical end force so $\gamma = 0.85$, $K_{\Theta} = 2.68$, $\eta = 1$, and $n = 0$. The length of the pseudo-rigid link is

$$\gamma l = (0.85)(0.18) = 0.153 \text{ in.} \quad (4.1)$$

The moment of inertia, I , is

$$I = \frac{wh^3}{12} = \frac{(0.25)(h)^3}{12} = 0.0208h^3 \quad (4.2)$$

The torsional spring constant, K , is found from Equation (3.20) as

$$K = \frac{\gamma K_{\Theta} EI}{l} = \frac{(0.85)(2.68)(200000)(0.0208h^3)}{0.18} = 52723h^3 \quad (4.3)$$

with $E = 200000 \text{ lb./in}^2$. The pseudo-rigid-body angle, Θ , is found from Equation (3.7) as

$$\Theta = \text{asin}\left(\frac{b}{\gamma l}\right) = \text{asin}\left(\frac{0.06}{0.153}\right) = 0.403 \text{ rad.} \quad (4.4)$$

The maximum force that the beam exerts on the ratchet occurs at the point of largest deflection in the free-wheeling direction. The maximum force that each pawl can exert on

the ratchet was specified to be $F = 0.16/3 = 0.053$ lb. With this value, the thickness of the beam, h , is now determined by combining Equation (3.12) and Equation (3.19) and solving for the force, F yields

$$F = \frac{K\Theta}{\eta\gamma l \sin\left(\frac{\pi}{2} - \Theta\right)} \quad (4.5)$$

substituting Equation (4.3) for K and solving for the thickness h results in

$$h = \sqrt[3]{\frac{F\eta\gamma l \sin\left(\frac{\pi}{2} - \Theta\right)}{52723\Theta}} = \sqrt[3]{\frac{(0.053)(1)(0.85)(0.18) \sin\left(\frac{\pi}{2} - 0.403\right)}{(52723)(0.403)}} = 0.0071 \text{ in.} \quad (4.6)$$

4.4.1.1 Test Results

Using CAD/CAM software the profile of the design was created, and tool paths were constructed. The clutch was manufactured using a prototyping mill. The device used to measure the free-wheeling and output torques was a hand-held digital strain gage meter and a torque sensor. An aluminum jig with a 9/32 in. hex head was attached to the clutch ratchet using four rivets. The reaction torque sensor was attached to the jig by a socket and a ratchet wrench was attached to the other end of the sensor. The least count for the torque sensor was 0.05 in.-lb. The sensor measured torque to the nearest 0.1 in.-lb. This indicates that there may be some error in the free-wheeling torque measurements, but for the output torques, as the torque increases, the effects of this possible error become negligible. It is assumed that any error in the free-wheeling torque measurement does not have any effect on the comparison ratios for the clutches because the torque measurement for each clutch contains the same error. This same apparatus is used to measure the torque for all of the

clutches. For this clutch the free-wheeling torque was measured at 0.1 in.-lb. The output torque measurement used for comparison is the peak static torque of the clutch before it fails. The peak static torque for this clutch was measured at 1.1 in.-lb. The ratio of free-wheeling torque to output torque for this clutch is 11.0. Table 4-2 shows the ratio of bending design 1 along with the torque ratios of the other clutch designs.

4.4.2 Bending Clutch Design 2

The next clutch, shown in Figure 4-5, incorporates the use of bending load of the pawls. As in the previous example, the pawls are slender cantilever beams that deflect away from the hub teeth in the free-wheeling direction. In the torque output direction, the

Table 4-2: Clutch torque ratio comparison

Clutch Type	Over-running Torque	Output Torque	Torque Ratio
Bending Design 1 (cantilever beam)	0.1 in.-lb.	1.1 in.-lb.	11.0
Bending Design 2 (cantilever beam with stiffening post)	0.2 in.-lb.	3.2 in.-lb.	16.0
Tension Design 1 (cantilever beam)	0.1 in.-lb.	44.0 in.-lb.	440.0
Tension Design 2 (slfp)	0.1 in.-lb.	82.0 in.-lb.	820.0
Compression Design 1 (cantilever beam)	0.1 in.-lb.	14.4 in.-lb.	144.0
Compression Design 2 (passive joint)	0.1 in.-lb.	581.0 in.-lb.	5810.0

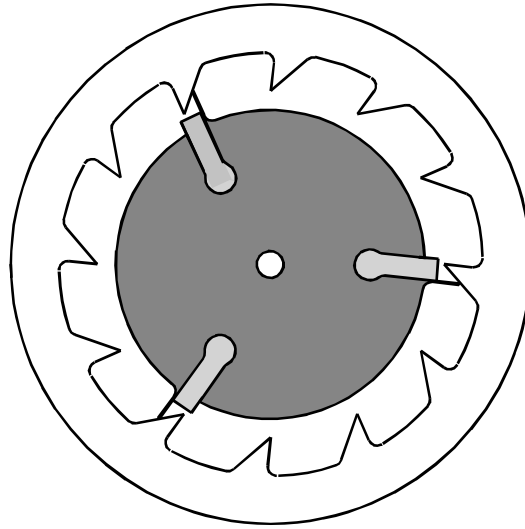


Figure 4-5 A compliant ratchet and pawl clutch with the pawls loaded in bending. The post serves to increase the stiffness of the beam in the torque output direction by decreasing the effective length of the cantilever beam.

hub tooth forces the cantilever beam to contact the post. The post stiffens the segment by reducing the effective length of the beam, and allows it to support a higher torque load.

The clutch will support torque loading until the beams yield and fold over. The PRBM for the pawl is also a cantilever beam. All parameters for this beam are the same as the previous example, including the segment thickness.

4.4.2.1 Test Results

The same methods discussed above were also used to prototype this clutch. The free-wheeling torque for this clutch was measured at 0.2 in.-lb. The peak static torque for this clutch was measured at 3.2 in.-lb. The ratio of free-wheeling torque to output torque for this clutch is 16.0. The increased output torque shows that the post aids in stiffening the beam, but the ratio does not increase by a significant amount. These designs show that loading the pawls in bending does not yield a high enough output torque to be of use. If the

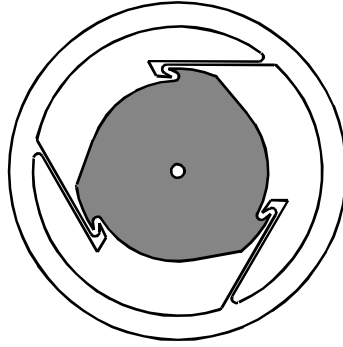


Figure 4-6 A compliant ratchet and pawl clutch with the pawls loaded in tension by the ratchet teeth.

stiffness of the beams is increased, the output torque will go up, but so will the free-wheeling torque, which is not a desirable consequence.

4.5 Tension Designs

This section discusses compliant ratchet and pawl clutch designs with the pawls loaded in tension in the torque output direction and bending in the free-wheeling direction. Two clutch designs were tested to determine their comparison ratios.

4.5.1 Tension Clutch Design 1

The first tension design uses a cantilever beam that is loaded in tension by the ratchet teeth that engage the pawls to provide a tensile loading. A diagram of this clutch is provided in Figure 4-6. In the free-wheeling direction, the pawl is deflected out of the way as the ratchet tooth passes by. The output torque is applied by the ratchet tooth engaging the tooth on the pawl. The pawl will support the torque until it reaches the point where the

pawl tooth yields and folds back out of the way allowing the ratchet tooth to slip out. The PRBM of the pawl is also a cantilever beam with a vertical end load. The parameters of beam, length, l , and deflection, b , were specified as 0.96 in. and 0.125 in., respectively, and the thickness, h , was solved for (see Figure 4-4). The values for n , η , K_{Θ} , and γ are the same as those for the above clutches. The torsional spring constant, K , was determined from Equation (4.3) as $K = 9887.2 h^3$. The pseudo-rigid-body angle, Θ , was found from Equation (4.4) as $\Theta = 0.154$ rad. Finally Equation (4.6) was solved for the segment thickness, h , yielding a thickness of 0.034 in. for the cantilever beams.

4.5.1.1 Test Results

After the clutch was prototyped, the torque tests were performed. The free-wheeling torque for the tension clutch was measured at 0.1 in.-lb., and the output torque was measured at 44.0 in.-lb. This type of pawl loading shows a large improvement in the peak static torque. The ratio of over-running torque to static torque is 440.0, which is clearly superior to the bending cantilever designs.

4.5.2 Tension Clutch Design 2

This clutch incorporates a different beam design than the previous three clutches. The pawls are loaded in tension when the ratchet teeth engage the pawl teeth in the torque output direction and deflect away from the ratchet teeth in the over-running direction. The pawls will support static torque until the pawls fail at the slender segments. The clutch is shown in Figure 4-7. The PRBM for the pawl is a small-length flexural pivot. Figure 4-8 shows the PRBM superimposed on the pawl. The design parameters that are independent

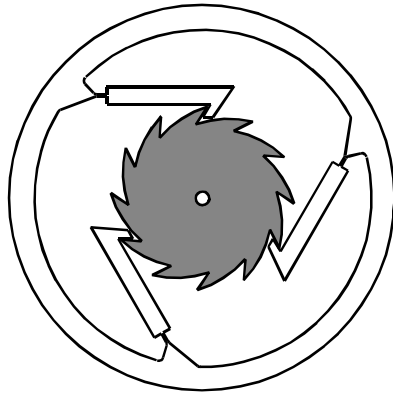


Figure 4-7 A compliant ratchet and pawl over-running clutch with small-length flexural pivots.

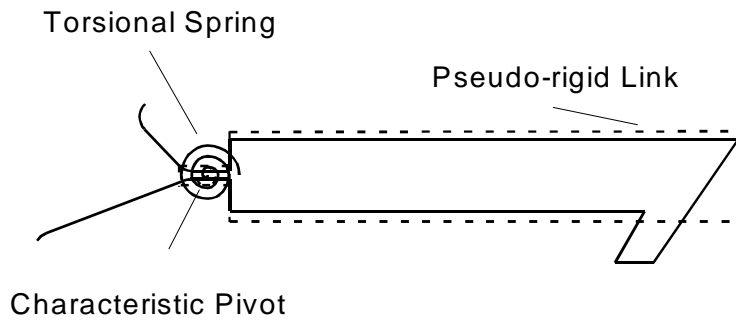


Figure 4-8 The PRBM of the small-length flexural pivot superimposed on the clutch pawl.

of the set criteria for all of the clutches are the length of the pawl, the length of the flexural pivot, the thickness of the pawl, and the distance the pawl will deflect to clear the ratchet

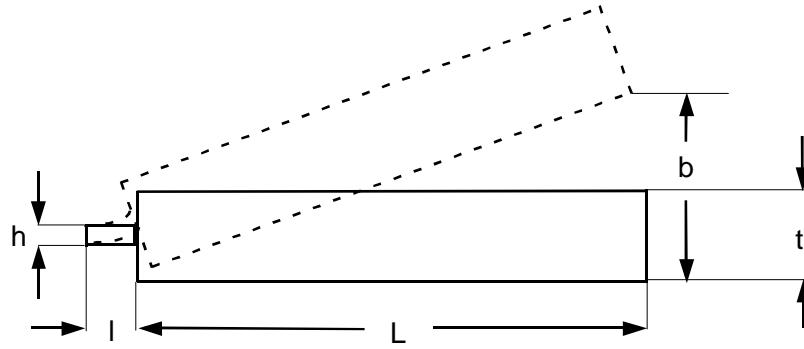


Figure 4-9 The dimensional parameters for the small-length flexural pivot and pawl.

tooth. Figure 4-9 shows the dimensional parameters for the slfp and the pawl. For this clutch, the length of the pawl, L , the length of the flexural pivot, l , the pawl thickness, t , and the deflection, b , were set at 1.0 in., 0.125 in., 0.1875 in., and 0.1875 in., respectively. Of all the listed parameters, the thickness of the pawl is the least important. The pawl only needs to be sufficiently stiff so that all of the flexure takes place in the flexural pivot. Since the beam is loaded with a vertical end force, the values for n , η , K_{Θ} , and γ remain the same as those from previous examples. From Equation (4.2) the moment of inertia, I , for the slfp (small-length flexural pivot) was found to be $I = 0.0208h^3$. The spring constant, K , is found from Equation (3.35) as

$$K = \frac{EI}{l} = \frac{(200000)(0.0208h^3)}{0.125} = 33328h^3 \quad (4.7)$$

The pseudo-rigid-body angle, Θ , is determined by

$$\Theta = \text{asin}\left(\frac{b}{L + \frac{l}{2}}\right) = \text{asin}\left(\frac{0.1875}{\left(1.0 + \frac{0.125}{2}\right)}\right) = 0.176 \text{ rad.} \quad (4.8)$$

The equation for the thickness of the slfp is found by substituting Equation (4.7) for K into Equation (4.5) and solving for h yielding

$$h = \sqrt[3]{\frac{\left(\left(L + \frac{l}{2}\right) \sin\left(\frac{\pi}{2} - \Theta\right) F\right)}{(33328)(\Theta)}} = \sqrt[3]{\frac{\left(\left(1 + \frac{0.125}{2}\right) \sin\left(\frac{\pi}{2} - 0.176\right) 0.053\right)}{(33328)(0.176)}} = 0.021 \text{ in. (4.9)}$$

4.5.2.1 Test Results

After constructing the clutch, the over-running and static torques were measured for the slfp pawl design and were found to be 0.1 in.-lb. in the free-wheeling direction and 82.0 in.-lb. in the torque output direction. These measurements produce a ratio of 820.0, which is the highest of the tension designs. The large increase in the torque ratio indicates that designs involving tension loading of the pawls may be feasible for some applications.

4.6 Compression Designs

This section presents compliant ratchet and pawl clutch designs with the pawls loaded in compression in the torque output direction. The preliminary theory and testing of two clutch designs is presented.

4.6.1 Compression Clutch Design 1

This design uses a cantilever beam for the pawl that is loaded in compression in the torque output direction and bending in the free-wheeling direction. The pawls are attached to the ratchet and the teeth are located on the outer hub. In the torque output

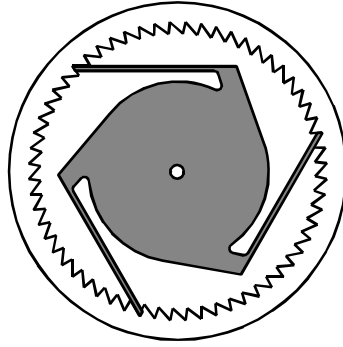


Figure 4-10 A compliant ratchet and pawl clutch with the pawls loaded in compression.

direction, the pawls engage the teeth on the hub. The pawl will support the torque loading until the critical load is reached and the beam buckles. The clutch is shown in Figure 4-10.

The PRBM for the pawl is also a cantilever beam. The equation describing buckling for a fixed-free Euler column is given as

$$P_{cr} = \frac{\pi^2 EI}{4L^2} \quad (4.10)$$

To achieve a high critical buckling load, it is necessary to have a large beam thickness, and a small column length. In order for the compliant segment to have a large thickness, it must also have a large length so that the stiffness remains within the given force constraint. For this application it was determined that the longest allowable beam would produce the largest segment thickness and thus the highest critical load. For this clutch, the beam length was found to be 1.5 in. The spring constant, K , and the pseudo-rigid-body angle, Θ , were found using the same methods described for earlier cantilever beam pawl designs and were determined to be $6327.8h^3$ and 0.098 rad., respectively. The segment thickness, h , was found from Equation (4.6) as $h = 0.048$ in.

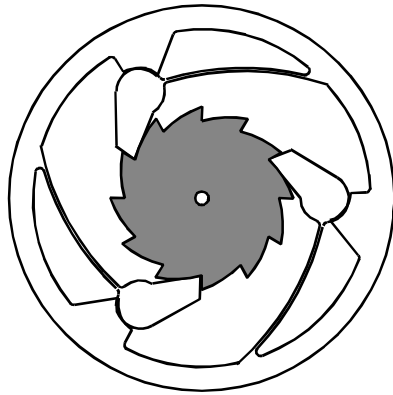


Figure 4-11 A compliant compression-loaded ratchet and pawl clutch (CCrat-pawl).

4.6.1.1 Test Results

The static torque tests for this clutch yielded 0.1 in.-lb. for the free-wheeling torque and 14.4 in.-lb. for the peak output torque. This gives a ratio of 144.0. It is interesting to note that this type of clutch has the least amount of backlash of any of the clutch types tested. This is due to the teeth being located on the hub instead of the ratchet.

4.6.2 Compression Clutch Design 2

In this clutch design, the pawls are loaded in compression in the torque output direction, and bending in the free-wheeling direction. The pawls are connected to compliant segments that provide the force to keep the pawls in contact with the ratchet. When the clutch free-wheels, the pawls rotate away from the ratchet as the teeth pass by. The pawl will support a torque loading in compression until the ratchet teeth fail. Figure 4-11 shows the compliant compression-loaded ratchet and pawl clutch (CCrat-pawl).

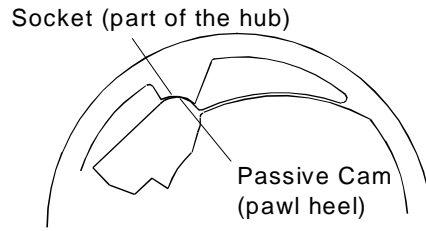


Figure 4-12 A passive joint showing the passive cam and socket.

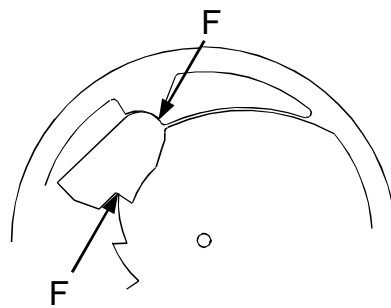


Figure 4-13 The diagram of compressive forces on the passive joint.

4.6.2.1 Passive Joints

An important factor in the design of this clutch is the use of passive joints to allow rotation of the pawls. A passive joint acts as a pin joint without requiring an actual pin. A passive joint is formed by combining a passive cam with a socket (see Figure 4-13). The motion is the same as a cam follower system with zero displacement. The application of a compressive load on the passive cam forces it into the socket and maintains it in that position, so that it has limited rotation about the center of the socket. In order for a passive joint to be substituted for a revolute joint, certain conditions must be met. First, as stated, the loading on the joint must be compressive. This ensures that the passive cam stays in

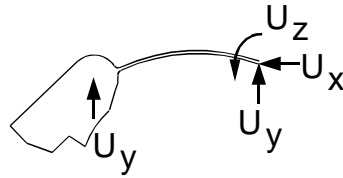


Figure 4-14 Pawl model with deflection constraints.

the socket. Second, a passive joint can only be used in those applications which do not require full rotation. Figure 4-13 shows a passive joint with applied compressive forces.

Although the PRBM method was not used to model the compliant segment, the model for the initially curved cantilever beam presented in Chapter 4 would also yield accurate results. The segment is assumed to undergo deflections in the linear regime where the linear deflection equations are valid. In order to determine the stiffness, the pawl and compliant segment were modeled with the initially curved segment being fixed in all degrees of freedom on the fixed side (where it joins the outer hub) and the pawl being allowed to rotate about the z -axis and fixed in the y direction (see Figure 4-14). Equations for the deflection of a cantilever circular arc (Young, 1989) were used to determine the moment about the passive joint and the force in the y direction. These equations yielded the following relations for the angular (β) and vertical (δy) deflections:

$$\beta = \frac{M_0 L}{EI} - \frac{R^2 F (2\psi \sin \psi)}{EI} \quad (4.11)$$

and

$$\delta y = \frac{R^2 M_0 2\psi \sin \psi}{EI} - \frac{R^3}{EI} [F (2\psi (\sin \psi)^2 + \psi - \sin \psi \cos \psi)] \quad (4.12)$$

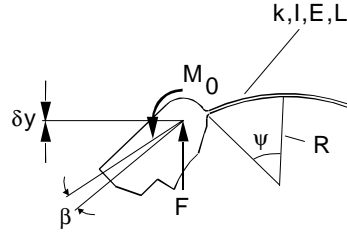


Figure 4-15 Model of the initially curved beam and pawl.

where L is the arc length, E the modulus of elasticity of the material, R the radius of curvature of the arc, ψ one half of the total subtended angle of the arc, and I the moment of inertia. F is the reaction force through the center of the passive joint, and M_0 is the moment caused by the angular deflection of the pawl about the passive joint. The model is provided in Figure 4-15. The vertical and angular deflections are specified with the vertical deflection (δy) set equal to zero, and the angular deflection (β) set equal to the desired angular deflection of the pawl. Substituting $I = wh^3/12$ into Equation (4.11) and Equation (4.12), and specifying the desired deflections and compliant segment parameters, the two simultaneous equations can then be solved to determine M_0 and h . These equations may also be manipulated to solve for other desired parameters. Having determined the moment, the stiffness of the beam can be calculated by using Equation (4.11) and Equation (4.12) to give

$$k = \frac{M_0}{\beta} = \frac{EI(2\psi(\sin \psi)^2 + \psi - \sin \psi \cos \psi)}{L(2 \sin \psi(\sin \psi)^2 + \psi - \sin \psi \cos \psi) - 4\psi^2(\sin \psi)^2 R}. \quad (4.13)$$

For this clutch, the force and segment width are already fixed. The parameters that can be specified by the designer are the desired angular deflection, the arc length, and the radius of curvature for the arc. The subtended angle of the arc will be specified by the arc length and radius of curvature. These parameters were chosen to be $\beta = 0.15$ rad., $L = 1.44$ in., and $R = 1.96$ in. making $\psi = 0.375$ rad. Substituting these parameters along with $I = 0.0208h^3$ and $F = 0.053$ lb. into Equation (4.11) and Equation (4.12) and solving the two simultaneous equations yields $M_0 = 0.051$ in.-lb. and $h = 0.031$ in. A finite element analysis model of the pawl and the compliant segment was also constructed with the same parameters and using $h = 0.031$ in. Nonlinear analysis was performed with 25 beam elements. The model produced results that correlate very well with the above equations, giving $M_0 = 0.0502$ in.-lb. and $F = 0.0527$ lb.

4.6.2.2 Test Results

After the clutch was manufactured, the free-wheeling and static torques were measured. The over-running torque for the CCrat-pawl clutch was measured at 0.1 in.-lb., and the peak static torque was measured at 581.0 in.-lb. This produces a ratio of peak static torque to over-running torque of 5810.0. This value is significantly larger than the ratios of the other clutches by factor of as much as 520 times the smallest ratio (bending pawl) and 7 times the largest ratio (pawl with slfp design).

Upon comparison of the ratios in Table 4-2, it is easily shown that the compliant ratchet and pawl clutch using compression loading of the pawls for torque output and compliant segments for free-wheeling is the best design to pursue. Examination of all of the clutch designs shows that in order to get a large output torque, the compliant segments should not be loaded in any manner. The compliant segments are a good choice to provide

the necessary force to keep the pawl in contact with the ratchet. The best combination is a rigid member to support the torque connected to a compliant member for free-wheeling. This is the type of design used in the second compression design that yielded the highest ratio. This compression clutch design will now be explored in further detail in Chapter 5.

Another interesting finding was the fair performance of the tension clutch using the slfp. In applications where the free-wheeling torque is not of great importance, the thickness of the slfp can be increased which will greatly increase the output torque. This may be a possible area for further research.

Further Development of the CCrat-pawl Clutch

In Chapter 4 it was shown that the compliant compression-loaded over-running ratchet and pawl clutch (CCrat-pawl) had the largest ratio of output torque to free-wheeling torque making it the best candidate solution. Some of the preliminary design theory was presented including the design of the compliant pawl segment and a brief discussion of the passive joints used in the clutch. In this chapter, further development of the theory needed to construct the clutch is presented along with a dynamic model for centrifugal throw-out of the pawls to reduce noise and wear. The issues of the design of the cam profile for the pawl, and the design of the passive joints are provided.

5.1 Design of the Cam Profile for the Pawl

The cam profile for the pawl is the surface that comes in contact with the ratchet tooth as it passes by. This profile is shown in Figure 5-1. The profile for the cam is the same profile as the ratchet tooth. This results in a solid, positive engagement of the pawl with the ratchet tooth. The most important design aspect of the profile is the position of the

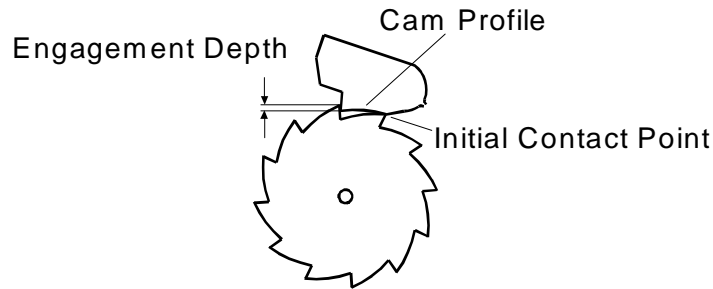


Figure 5-1 Diagram of the cam profile, the initial contact point, and the engagement depth of the pawl tooth into a ratchet tooth,.

initial contact point. The location of this point is the determining factor in the engagement depth of the pawl tooth. Engagement depth (see Figure 5-1) refers to the distance that the pawl tooth drops to contact the ratchet tooth in engagement. The noise that the clutch makes when it free-wheels is influenced by the distance the pawl drops from the point where it slides over the tip of the ratchet tooth to the point where it comes to rest on the ratchet. To achieve complete engagement, it is desirable to have the entire pawl tooth engaged with the ratchet tooth, but this requires a large engagement depth. To reduce the noise, the engagement depth must be as small as possible. Also, as the engagement depth is increased, the free-wheeling torque is also increased because the pawl must rotate farther to allow the ratchet tooth to pass by. Due to the contradictory nature of these two constraints, other factors must be addressed to determine the amount of engagement depth necessary. If clutch noise and free-wheeling torque do not have a large impact in the application, then a large engagement depth would be the best choice. However, if clutch noise and free-wheeling torque must be kept at the lowest value possible, a very shallow engagement depth would be necessary. One of the added benefits of the passive joint is to allow the pawl to rotate not only away from the pawl to free-wheel, but the pawl is also free to rotate into more complete engagement even with a shallow engagement depth. One

problem with making the engagement depth too shallow is that the pawls will skip over the teeth if the distance is too small and will not engage at all. For the example clutch discussed above, an engagement depth of 0.0625 in. was satisfactory to yield complete engagement and low free-wheeling torque.

5.2 Design of Passive Joints

The passive joint used in the construction of the clutch was introduced in Chapter 5. The passive joint allows the pawl to rotate and act as if it were pinned. For this clutch, the remaining design considerations for the passive joint are its location and the profile of the passive socket.

The location of the passive socket is dependent upon the pawl and its attached compliant segment. For this clutch the pawl had to be constructed in a position away from the passive socket to allow the cutting tool sufficient space to cut the contour of the passive socket and the contour of the pawl. The pawl heel and the passive socket should have the same radius of curvature to ensure a close fit. The passive socket was first constructed with the pawl in the desired position for operation. Using the PRBM for an initially curved segment with an applied end force, Equation (3.25) and Equation (3.26) can be solved for the coordinates of the deflected end point of the beam for manufacturing. For the example above it was necessary to have a 0.1 in. gap between the passive socket and the pawl to allow a 0.09375 in. diameter end mill to pass through. As shown in Figure 5-2, the pawl was modeled as an initially curved end-loaded cantilever beam with the rigid

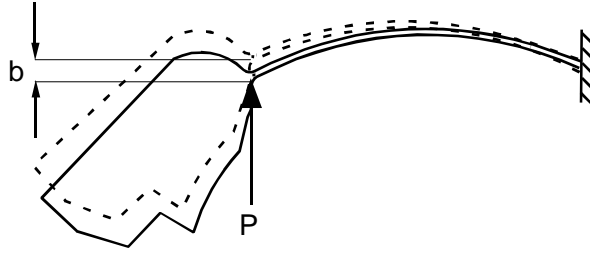


Figure 5-2 Clutch pawl modeled as an initially curved end-loaded cantilever beam.

pawl attached to the beam end. In order for the tool to clear the gap, the beam must have a vertical deflection of $b = 0.1$ in. The nondimensionalized parameter

$$\kappa_0 = \frac{L}{R} = \frac{(1.44in)}{(1.96in)} = 0.735 \quad (5.1)$$

The translated initial coordinates of the beam end are $a_i = 1.432$ in. and $b_i = 0.14$ in. and $\gamma = 0.81$. The characteristic radius is

$$\rho = \left[\left(\frac{a_i}{L} - (1 - \gamma) \right)^2 + \left(\frac{b_i}{L} \right)^2 \right]^{\frac{1}{2}} = \left[\left(\frac{1.432in}{1.44in} - (1 - 0.81) \right)^2 + \left(\frac{0.14in}{1.44in} \right)^2 \right]^{\frac{1}{2}} = 0.81 \quad (5.2)$$

the pseudo-rigid body angle, Θ , can be found from Equation (3.26) since the vertical deflection is given:

$$\Theta = \text{asin} \left(\frac{b}{\rho L} \right) = \text{asin} \left(\frac{0.1in}{(0.81)(1.44in)} \right) = 0.086 \text{ rad.} \quad (5.3)$$

The deflected horizontal coordinate, a , may be found from Equation (3.25) as

$$a = L(1 - \gamma + \rho \cos \Theta) = 1.44in(1 - 0.81 + 0.81 \cos(0.086rad)) = 1.436 \text{ in.} \quad (5.4)$$

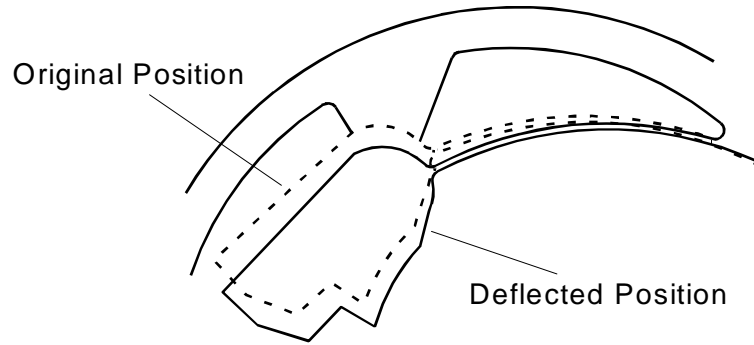


Figure 5-3 The clutch pawl shown in its normal operating position (original position) and in its deflected position for manufacturing.

The change in the horizontal coordinate is $1.44 \text{ in.} - 1.436 \text{ in.} = 0.0043 \text{ in.}$ With these changes applied to the original coordinates, the required location of the beam end is now known, and the pawl can now be placed at this position on the CAD drawing so that when the clutch is manufactured, the pawl can be deflected to the appropriate position where the pawl heel is seated in the passive socket for normal operation. The pawl in its original and deflected position for machining are shown in Figure 5-3.

5.3 Dynamic Model for Centrifugal Throw-out

A dynamic model to predict the rotational speed of the clutch required for centrifugal throw-out of the pawls has been developed. Centrifugal throw-out of the pawls helps to reduce noise and wear. This model may also be used to design the compliant segment of the clutch for throw-out at a desired rotational velocity. The model assumes that the passive joint acts like a fixed pin joint. Figure 5-4 shows a diagram of the model. The moment on the pawl about the pin joint is given as

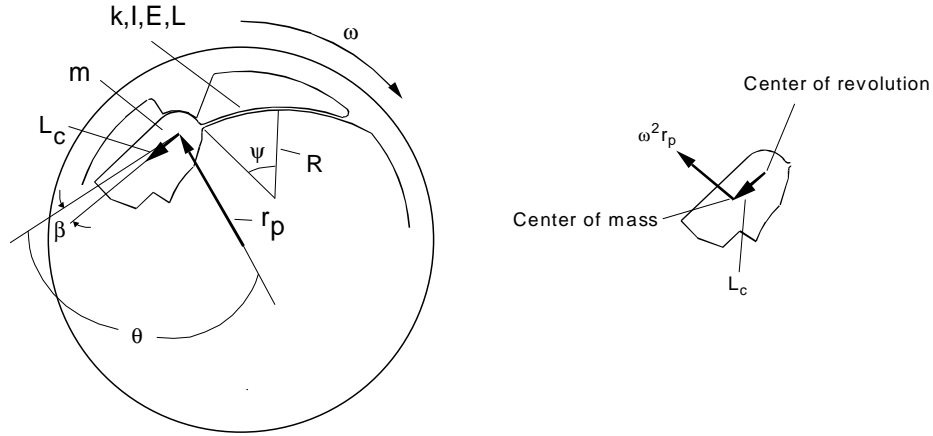


Figure 5-4 The dynamic clutch model for centrifugal throw-out of the pawls.

$$M_0 = k\beta \quad (5.5)$$

where k is the stiffness for the compliant segment and β the angle, in radians, that the pawl rotates to clear the ratchet tooth. The segment is assumed to undergo deflections in the linear regime where the linear deflection equations are valid. To determine the stiffness, the pawl and compliant segment were modeled using Equation (4.11) and Equation (4.12). As shown in the previous chapter, these two simultaneous equations can be solved to determine M_0 and F . Having found the moment, Equation (4.13) can be used to determine the stiffness of the segment. The moment on the pawl due to the centrifugal force is defined as

$$M_0 = \omega^2 L_c r_p m \sin \theta \quad (5.6)$$

with ω the angular velocity, L_c the vector from the center of the passive joint to the center of mass, r_p the vector from the center of the clutch to the center of the passive joint, m the

$$M_0 = \omega^2 L_c r_p m \sin \theta \text{ (Nm)}$$

$$\theta_0 = \text{(rad, angle between } r_p \text{ and } L_c)$$

$$k = \frac{EI(2\psi(\sin\psi)^2 + \psi - \sin\psi\cos\psi)}{L(2\sin\psi(\sin\psi)^2 + \psi - \sin\psi\cos\psi) - 4\psi y^2(\sin\psi)^2 R}$$

$$E = \text{(Pa, modulus of elasticity)}$$

$$L = \text{(m, arc length)}$$

$$R = \text{(m, radius of curvature of the arc)}$$

$$\psi = \text{(rad, one half of the arc angle)}$$

$$I = \frac{bh^3}{12} \quad (\text{m}^4, \text{moment of inertia})$$

$$b = \text{(m, material width)}$$

$$h = \text{(m, material thickness)}$$

$$\beta = \text{(rad, rotation of pawl away from ratchet teeth)}$$

$$\theta = \beta + \theta_0 \text{ (rad)}$$

$$M_0 = k(\theta - \theta_0) \text{ (Nm)}$$

$$L_c = \text{(m, distance from center of rotation to the center of mass)}$$

$$r_p = \text{(m, distance from center of clutch to center the of rotation)}$$

$$m = \text{(kg, mass of pawl)}$$

$$\omega = \text{(rad/s, angular velocity)}$$

Figure 5-5 Mathematical model for centrifugal throw-out of pawls.

mass of the pawl, and θ the angle between r_p and the position of the pawl when it is fully rotated by the ratchet tooth sliding by (refer to Figure 5-4).

Equation solving software was used to solve the multiple equations. The mathematical model of equations is provided in Figure 5-5.

5.3.1 Example

With the above equations, it is now possible to solve for several different variables.

For example, a given clutch has the following specified parameters:

For the compliant segment:

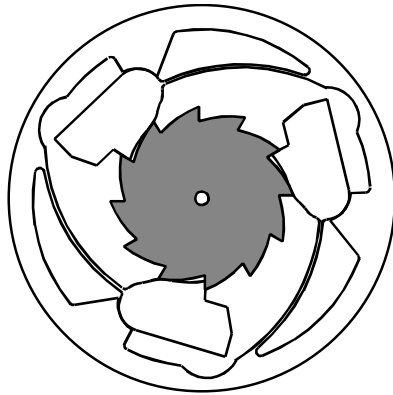


Figure 5-6 A compliant over-running ratchet and pawl clutch with centrifugal throw-out.

$$L = 36.6 \text{ mm (1.44 in.)}$$

$$R = 49.8 \text{ mm (1.96 in.)}$$

$$\psi = 0.375 \text{ rad.}$$

$$h = 0.794 \text{ mm (0.03125 in.)}$$

$$b = 6.35 \text{ mm (0.25 in.)}$$

$$I = 0.223 \text{ mm}^4 (6.358 \times 10^{-7} \text{ in}^4.)$$

$$E = 1.39 \text{ GPa (polypropylene) (200,000 lb./in}^2.)$$

For the pawl:

$$m = 2.222 \text{ g (} 4.9 \times 10^{-3} \text{ lb.)}$$

$$L_c = 9.09 \text{ mm (0.358 in.)}$$

$$r_p = 31.2 \text{ mm (1.23 in.)}$$

$$\theta = 1.31 \text{ rad.}$$

The required angular deflection for the pawls to clear the ratchet teeth is 0.149 radians. Figure 5-6 shows the example clutch. Equation (4.11) and Equation (4.12) were solved to yield the moment and force values of $M_0 = 5.663 \times 10^{-3} \text{ N}\cdot\text{m}$ (0.0501 lb-in)

and $F = 0.233 \text{ N}$ (0.0524 lb). A finite element analysis model of the pawl and the compliant segment was also constructed with the same parameters. It produced results that correlate with the above equations, giving $M_0 = 5.672 \times 10^{-3} \text{ N-m}$ (0.0502 lb-in) and $F = 0.234 \text{ N}$ (0.0527 lb).

Using these results, Equation (4.13) was solved for the spring constant which was found to be $k = 0.038 \text{ N-m}$ (0.337 lb-in). Equation (5.5) can now be set equal to Equation (5.6) and the angular velocity required for the pawls to rotate until they are no longer in contact with the ratchet teeth can be determined. The angular velocity for the pawls to be released to the tip of the ratchet teeth is predicted to be 910 rpm. The equations in Figure 5-5 can also be manipulated to solve for other parameters. For example, a compliant segment can be designed for a given throw-out velocity.

5.3.2 Test Results

The methods discussed above were also further investigated by designing, fabricating and testing a compliant over-running clutch and comparing test results to predicted performance. The test clutch was built to the specifications listed above.

The clutch was constructed using CAD software to draft the clutch profile and an NC mill was used to manufacture the hub and the ratchet. The profile for the clutch is provided in Figure 5-7. The gap that exists between the heel of the pawl and the socket of the passive joint is due to the distance necessary to allow the cutting tool to follow the contour without gouging the hub. This distance can be greatly reduced by using manufacturing methods such as injection molding, laser, water jet cutting, or wire EDM.

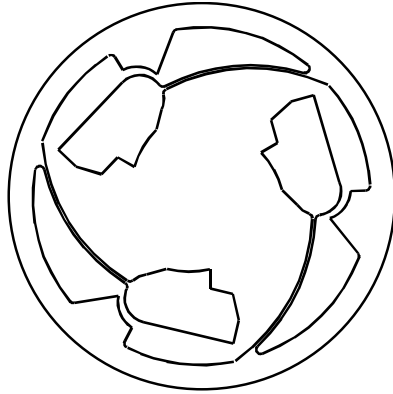


Figure 5-7 The CAD profile of the compliant over-running clutch with centrifugal throw-out.

The model was used to predict the angular velocity required to rotate the pawls so that they would be a radial distance from the tip of the ratchet teeth of 0.397 mm (0.0156 in) at 975 rpm and 1.59 mm (0.0625 in) at 1047 rpm. An experimental set up was then used to verify that the tip of the pawl displaced the predicted distance for a given angular velocity. The clutch hub was placed in the chuck of a NC lathe such that the angular velocity could be controlled. The ratchet was held fixed by a chuck in the tail stock and was not allowed to rotate. Two lines were scribed into the hub at distances of 0.397 mm (0.0156 in) and 1.59 mm (0.0625 in). A strobe light was used to measure the angular velocity of the chuck. The location of the pawl relative to the scribed lines was determined visually at the calculated angular velocities. The worst case measurement error is one line width on either side of the scribed line. Including the maximum possible error, the predicted results were within 5.2% of the experimental results at both speeds tested (975 and 1047 rpm). It is believed that this error would be reduced by using a more accurate measuring method.

In Chapters 5 and 6, the governing design theory for the chosen over-running ratchet and pawl clutch was presented. However, several key design issues must be addressed in the initial design phase of a compliant over-running clutch. Many of the decisions are based on the desired application and the service loads. For example, the allowable diameters for the hub and the ratchet determine the size and the number of pawls that may be used. The loading determines the number of pawls necessary to support the load. The desired precision or the amount of acceptable backlash determines the offset of the pawls and the number of teeth on the ratchet. This chapter contains an investigation into these issues and other issues including manufacturing, material selection, backlash and wear, fatigue, static failure, and designing a clutch for a given output torque.

6.1 Manufacturing

One of the advantages of compliant mechanisms is the possible reduction in manufacturing time and cost. Various manufacturing methods may be used to construct

compliant over-running clutches. For polymer materials, as described above, an inexpensive method for high volume manufacturing would be injection molding. Extrusion may also be an alternative manufacturing method, although the polymers may not be optimally aligned. Aluminum or steel clutches may be manufactured using laser, water jet cutting, wire EDM or NC milling. An example of one of these alternative manufacturing methods (wire EDM) is discussed later.

6.2 Material Selection

Several materials may be used in the design and construction of compliant over-running clutches. Polymers are an attractive choice because they are relatively inexpensive and can be used in high volume manufacturing processes such as injection molding. Self-lubricating polymers can be used to reduce the need for lubrication and also reduce wear. A disadvantage to using polymers is the loss in strength.

For higher strength, steel or aluminum can be used. Although these materials have the advantage of high strength, the manufacturing methods used would increase the cost. However, the overall advantages of reduced assembly and maintenance of joints would still apply.

Materials with a high ratio of strength to Young's modulus are good candidates for compliant mechanisms. If Young's modulus for the material is low, the material can deflect with minimal forces. If the strength is high, the material can support large deflections before failure. Strength to modulus ratios for several materials are provided in Table 6-1. Polypropylene is an attractive material for use in compliant mechanisms because it has a very high ratio of strength to Young's modulus as compared to other materials. All of

the test clutches presented thus far were constructed from polypropylene. Nevertheless, polypropylene is not the only possible material choice. For test purposes a compliant ratchet and pawl clutch was constructed from T-6061 Aluminum. The clutch was manufactured using wire EDM to construct the outer hub and NC milling to construct the ratchet and back plate. Wire EDM was used because of the very small thickness of the compliant segment, and the small clearance between the socket on the hub and the passive cam (pawl heel). The aluminum clutch is shown in Figure 6-1.

The design constraints from the previously tested clutches were also used to design this clutch. The thickness of the compliant segment was $h = 0.0084$ in. The drawback to using materials such as aluminum and steel is that their ratio of strength to Young's modulus is not as high. This translates into compliant segments with very small thicknesses which are subject to permanent deformation by yielding. Although these materials exhibit this weakness, if the allowable over-running torque can be increased, the thickness of the compliant segments can be increased resulting in a more robust clutch. The clutch performance in terms of peak static torque also easily out performs those clutches constructed from polymer materials.

Table 6-1: Material strength to Young's modulus ratios

Material	Yield Strength (lb./in. ²)	Young's Modulus (lb./in. ²)	Ratio
Polypropylene	4600	200000	0.023
Aluminum T-6061	40000	9.975×10^6	0.00401
Steel AISI 1040 CD	71000	30.0×10^6	0.00237
Polysilicon	174000	24.7×10^6	0.0071

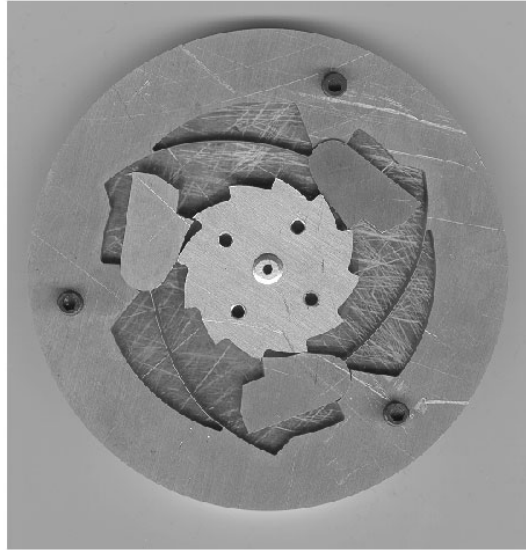


Figure 6-1 An aluminum over-running compliant ratchet and pawl clutch with centrifugal throw-out.

6.3 Backlash

A common problem faced by ratchet and pawl clutches is that of backlash. Backlash occurs when the clutch is reversed from a free-wheeling direction to a torque output direction. Because there is a limited number of positions where the pawls can engage, the ratchet rotates a small distance before engagement. In some applications this is not a problem. For those cases where it is desirable to minimize the backlash there exist several solutions. For example, the ratchet can be designed to contain a higher number of teeth, or the pawls in the hub can be offset so that only one pawl engages. An example of a compliant ratchet and pawl clutch with offset pawls is shown in Figure 6-2. Additional pawls can also be added to the hub to reduce backlash if size constraints allow it. The

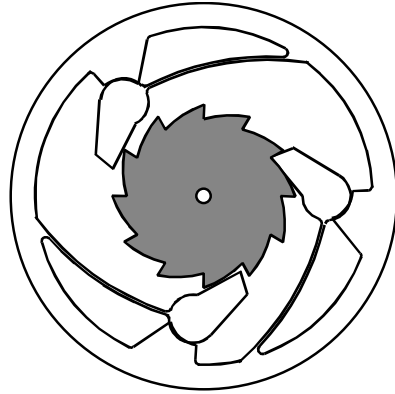


Figure 6-2 A compliant over-running ratchet and pawl clutch with the pawls offset to reduce backlash.

ratchet gear itself may be modified to reduce backlash. By increasing the number of teeth on the gear, the backlash is reduced. However, this change may require a change in the pawl design so that the pawl teeth and the ratchet teeth continue to engage properly. It is also important to consider the loads that the clutch is required to support because this has a large effect on the number of pawls required to handle the loading.

6.4 Wear

Another important consideration in the design of over-running clutches is the inherent wear in the system. Sliding friction is the greatest source of wear in the pawls and the ratchet teeth. The wear in these areas may be reduced by using centrifugal forces to rotate the pawls away from the ratchet when free-wheeling. Even at angular velocities below the velocity required for complete release, the wear is reduced because the smaller centrifugal force developed by the rotation reduces the normal force of the pawls against the ratchet teeth and thus the friction. This design feature reduces overall wear and extends the life of the clutch. Wear is also reduced in the compliant ratchet and pawl clutch

because it does not rely on friction for engagement as do roller and sprag clutches. Lubrication is also not as critical as it is for the sprag and roller clutches (South and Mancuso, 1994).

The amount of wear is dependent upon several factors. The application of the clutch (including torque loading), materials used in construction, operational over-running velocities, temperature, and the forces on the system (compliant segment stiffness). All of these parameters change from application to application. According to Kragelsky et al., 1982, wear also varies according to surface pressure, surface finish and surface films. This means that wear and fatigue must be evaluated for each situation.

6.5 Fatigue

Fatigue is an important design issue in compliant mechanisms because the compliant segments are often subjected to alternating loads. The compliant segments in the over-running clutch are subjected to alternating loads due to the moment applied on the segment by the pawl as the ratchet tooth passes by. As each ratchet tooth passes by the pawl tooth in the over-running direction, the pawl is first deflected away, and then is brought back into contact with the ratchet. Depending on the number of ratchet teeth and the angular velocity of the clutch, this alternate loading may take place at a very high cyclic rate. Fatigue calculations are much more simple for materials such as steel or aluminum, and much information is available. For materials such as polymers, there are many factors that must be considered which make the normally simple fatigue predictions very difficult. Predictions for the fatigue strength of two compliant ratchet and pawl clutch designs are provided along with a brief investigation into the fatigue of the polypropylene

clutch. All clutches were designed using the design criteria from Chapter 5. A finite element model of the beam was constructed to determine the maximum stress in the compliant segment at the point where the pawl slips over the ratchet tooth. The compliant segment was modeled as two structural 2-D elastic beams joined together. One beam modeled the flexible segment and the other beam modeled the rigid pawl. The rigid beam was divided into five elements and the flexible beam was divided into 20 elements for meshing. A copy of the finite element model batch file is provided in Appendix A. The fatigue predictions that follow for the aluminum and steel clutches and the test that was performed on a polypropylene clutch only include half of the deflection path of the pawl. Nevertheless, they do provide insight to the cycle life of the clutch.

6.5.1 Aluminum Clutch Example

For an aluminum clutch manufactured using 7075-T6 aluminum the ultimate tensile strength is 82,000 lb./in.² The maximum stress in the segment was found to be approximately 23,700 lb./in.², and the minimum stress was 0.0 lb./in.². Using the fatigue strength diagram for 7075-T6 aluminum provided in Juvinall, 1967, the fatigue strength was determined to be on the order of greater than 1.0×10^9 cycles. Although aluminum does not have an endurance limit, a value of 5×10^8 cycles may be considered infinite life. Juvinall, 1967, provided the equation for the endurance strength as

$$S_n' = 0.4S_u = (0.4)(82000) = 32800 \frac{lb}{in^2} \quad (6.1)$$

where S_u is the ultimate tensile strength. The maximum stress in the segment is less than

the endurance strength indicating infinite life which also corresponds with the fatigue strength diagram.

6.5.2 Steel Clutch Example

Next, a compliant steel clutch was evaluated. The clutch material was chosen to be AISI 1040 cold drawn steel with an ultimate tensile strength of 85,000 lb./in.² and a yield strength of 71,000 lb./in.². From Juvinall, 1967, the 10³-cycle strength for bending is given as

$$S = 0.9S_u = (0.9)(85000) = 76500 \frac{lb}{in^2}. \quad (6.2)$$

The endurance limit for steel is approximated by

$$S_n' \approx 0.5S_u = (0.5)(85000) = 42500 \frac{lb}{in^2}. \quad (6.3)$$

The 10⁶-cycle strength is found from

$$S_n = S_n' C_L C_D C_S = (42500)(1.0)(1.0)(0.78) = 33150 \frac{lb}{in^2} \quad (6.4)$$

where C_L is the load constant equal to 1.0 for bending, C_D is the size factor equal to 1.0 for the part diameter < 0.4 in., and C_S is the surface factor equal to 0.78 for a machined surface with a Bhn = 170. With the 10³-cycle strength and the 10⁶-cycle strength, a $S-N$ curve can be constructed to predict the fatigue life of the clutch. The $S-N$ curve is shown in Fig-

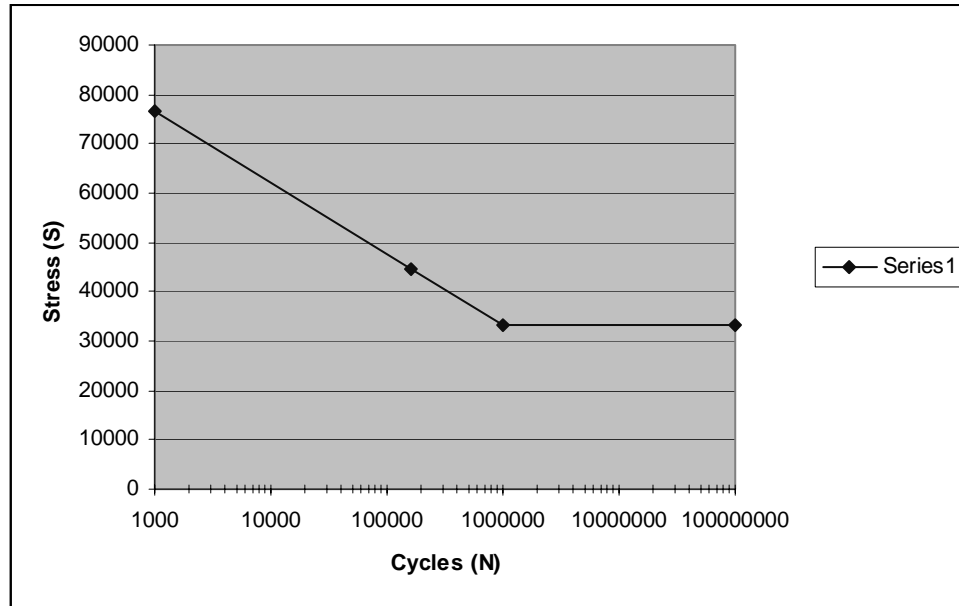


Figure 6-3 S-N curve for AISI 1040 CD steel.

ure 6-3. The maximum stress for the compliant segment is approximately 44700 lb./in.². This stress is above the endurance limit and is plotted in Figure 6-3 yielding a predicted fatigue life of 158740 cycles. In order to design a clutch that would have infinite fatigue life, the maximum stress would have to be below 33150 lb./in.². The required thickness of the compliant segment to reduce the stress to this level is 0.004 in. as compared to the original thickness of 0.0059 in. At this thickness, the maximum stress is 30000 lb./in.² resulting in infinite life.

This fatigue prediction show the weakness of using steel as a material for designing compliant mechanisms. For the beam to exhibit infinite life in fatigue the beam thickness had to be reduced to the point where the structural integrity of the clutch is compromised. At such a small thickness, the compliant segment may be easily damaged to the point where the clutch will no longer perform as designed.

6.5.3 Testing of a Polypropylene Clutch

A test was performed on the polypropylene compliant clutch to show that although the fatigue life of the compliant segments is difficult to predict, an actual measurement provides some idea of the clutch life. The clutch hub was placed in the chuck of a NC lathe such that the angular velocity could be controlled. The ratchet was held fixed by a chuck in the tail stock and was not allowed to rotate. A strobe light was used to measure the angular velocity of the chuck. The test was run with the chuck of the lathe rotating at 1100 rpm. After one hour the lathe was stopped to see if there was any noticeable thermal increase in the compliant segments. No noticeable increase in temperature was evident. The test was allowed to run for a continuous period of 16 hours. Once again no noticeable increase in temperature was detected. Some visible wear was present on the lower ratchet teeth due to misalignment of the tail stock with the chuck. The test was continued and finally stopped at 1.0×10^8 cycles. A desirable number of cycles to indicate infinite life would be 5×10^8 cycles. For this test, this would require almost 27 days of continuous operation of the clutch to reach this many cycles. The finite element model yielded a value of 1700 lb./in.^2 for the maximum stress which is considerably lower than the yield stress of 4600 lb./in.^2 .

6.6 Static Failure

Failure modes for the compliant clutch were investigated to determine the weaknesses of the clutch and to illuminate those areas where the device can be improved to increase the overall performance.

In static torque testing the first failure mode for the clutch was ductile failure of the ratchet teeth. The torque reached a maximum where one of the three engaged ratchet teeth sheared off. After the tooth failed, the ratchet would rotate and shear the pawl off where it joined the compliant segment. This failure mode was the same in all of the specimens tested.

To determine the second failure mode the material of the ratchet was changed so that the ratchet would no longer be a source of failure. The ratchet gear was constructed from T-6061 aluminum and the static torque test was performed once again. As was expected, the clutch now failed in ductile failure of the pawl teeth. The torque reached a maximum where the aluminum ratchet teeth sheared off the polypropylene pawl teeth.

Changing the material of the ratchet from polypropylene to aluminum did serve to increase the output torque. In the two static tests performed, one clutch failed at 602.0 in.-lb. and the other clutch failed at 620.0 in.-lb. This is an increase in torque capacity of a minimum of 3.5% and a maximum of 6.3%. This is not as large of an increase as was expected. To increase the strength of the pawl teeth, the tooth size must be increased and the engagement depth must be increased to allow a larger tooth to completely engage the ratchet tooth. However, this improvement does not come without a cost. As discussed in Chapter 6, increasing the engagement depth also increases the noise, and the over-running torque of the clutch.

6.7 Designing a Clutch for a Given Output Torque

Given a desired output torque, a CCrat-pawl clutch can be designed to support the load. The process to design a clutch for a given minimum output torque requires that

certain initial decisions be made. The type of material, number of pawls and the engagement depth are the most important decisions to be made. The number of pawls determines how much force each pawl is to support. The engagement depth determines the area that the force acts on. The force divided by the area (engagement depth x material thickness) yields the stress on the pawl tooth and the clutch tooth. This stress should be lower than the yield strength of the material to prevent failure. If this stress is higher than the yield strength of the material, one or more of the following could be done: a different material could be used, more pawls could be added, or the effective area could be increased by increasing the thickness of the material or increasing the engagement depth.

Other decisions that affect the clutch design are the allowable over-running torque (this determines the compliant segment thickness), the desired velocity for throw-out of the pawls (this determines the pawl size and location of the required center of gravity for the pawl), and the allowable clutch diameter (this effects the number of allowable pawls).

With these decisions made, a clutch that supports the desired output torque can be designed.

6.7.1 Example

For example, a CCrat-pawl clutch is to be designed to support an output torque of 2000 in.-lb. Three pawls are to be used in the design. This requires that each pawl support approximately 670 in.-lb. of torque. The engagement depth is set at 0.125 in. The material thickness is given as 0.25 in. The effective area is

$$A = bh = (0.125)(0.25) = 0.03125 \text{ in.} \quad (6.5)$$

The ratchet for the clutch is the same ratchet described for the CCrat-pawl clutch in Chapter 4. The distance from the center of the ratchet gear to the center of the effective area is 0.9375 in. The force exerted on the ratchet tooth is

$$F = \frac{T}{r} = \frac{(670)}{(0.9375)} = 714.7 \text{ lb.} \quad (6.6)$$

The stress is given as

$$\sigma = \frac{F}{A} = \frac{(714.7)}{(0.03125)} = 22870 \text{ lb./in.}^2 \quad (6.7)$$

This value of stress is greater than the yield strength for polypropylene so it cannot be used to construct the clutch without modifying the clutch geometry. The yield strength for T-6061 aluminum is 40000 lb./in.². The stress is less than the yield strength for this material so it may be used to construct the clutch and support the desired load.

The compliant ratchet and pawl clutch is a viable alternative to the traditional rigid-body ratchet and pawl clutch which means that it can be used in many of the same applications that now only incorporate rigid-body clutches. The next chapter discusses a comparison of the CCrat-pawl clutch to its traditional rigid-body counterpart.

Comparison of Compliant and Traditional Clutches

With a completed design of the CCrat-pawl clutch accomplished, the clutch can now be compared to its traditional rigid-body counterpart to determine its overall strengths and weakness. The two clutches are compared using the following criteria: manufacturing time, assembly, part count, peak static torque, clutch weight, and fatigue.

7.1 Manufacturing Time

For a manufacturing time comparison, the ratchet and pawl clutch with centrifugal throw-out and a traditional rigid-body ratchet and pawl clutch were constructed using the same NC prototyping mill. Their machining times were measured for comparison. The rigid-body ratchet and pawl clutch is shown in Figure 7-1. The clutch was designed using the same design constraints presented earlier for the number of pawls, allowable force on the ratchet, material, and the allowable outer diameter. The spindle speed and material feed rate were kept at the same settings for both clutches. The compliant clutch required 18.0 minutes to manufacture including a manual tool change. The rigid-body clutch



Figure 7-1 A traditional rigid-body ratchet and pawl clutch.

required 45.5 minutes. This demonstrates the possibility for large savings in time and money for manufacturing the compliant clutch. If injection molding is considered for the polypropylene clutch, the savings in time and money are increased even more because of the high volumes possible.

7.2 Assembly and Part Count

In order to compare assembly and part count of the two clutches, both clutches were first completely disassembled. Figure 7-2 and Figure 7-3 show the parts for the rigid-body clutch and the compliant clutch. It is easy to see that the rigid-body clutch requires considerable assembly. First, the leaf springs are put into their position in the outer hub. Next, the pawls are attached to the hub by the pins. Fasteners are used to keep the pins in place. Finally, the ratchet gear is attached to the hub with a pin. In comparison, the only

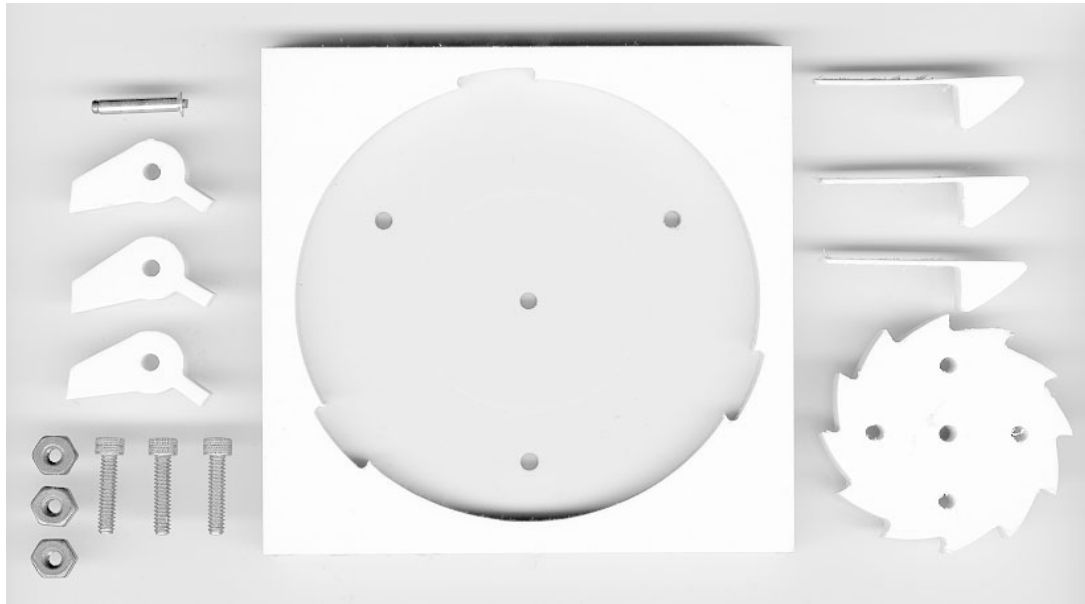


Figure 7-2 Disassembled rigid-body ratchet and pawl clutch.

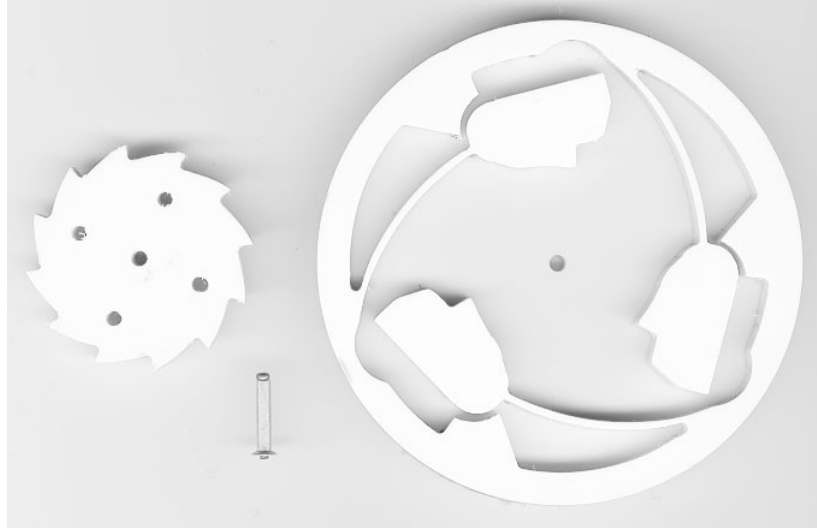


Figure 7-3 Disassembled compliant ratchet and pawl clutch.

assembly the compliant clutch requires is to attach the ratchet gear to the hub with the pin. Assembly times were not measured because upon visual inspection of the parts it may be determined that the rigid-body clutch requires a greater amount of time to assemble.

Examination of both clutches shows how much the part count has been reduced through the use of compliance. Excluding the ratchet gear and pin, the rigid-body clutch has a minimum part count of 13. The compliant clutch has a part count of only 1. This demonstrates a dramatic reduction in part count through the use of compliance.

7.3 Peak Static Torque

As mentioned earlier, the peak static torque for the compliant clutch was measured at 581.0 in.-lb. The peak static torque for the rigid-body ratchet and pawl clutch was measured at 641.0 in.-lb. The traditional clutch failed in the ratchet teeth at peak torque. The peak torque is higher in the traditional clutch due to a larger engagement depth. For a compliant clutch with the same engagement depth the peak torque should be the same as that of the traditional rigid-body clutch because both clutches are loaded in compression and fail in the same manner. This comparison of peak torque between the two clutches shows that both clutches are relatively equal in their peak torque capacity.

7.4 Clutch Weight

The overall weight of the compliant clutch and the rigid-body clutch were compared to determine if the use of compliance results in any significant savings in the amount of material required for construction. Two versions of the compliant clutch were weighed. The first version was the CCrat-pawl clutch with centrifugal throw-out. The second compliant clutch was the CCrat-pawl clutch without centrifugal throw-out. The result of not incorporating centrifugal throw-out is a savings in material accomplished through the use of smaller pawls. All clutches were weighed without the ratchet being

included. The rigid-body clutch weighed 95.4 grams. The compliant clutches weighed 93.2 grams and 90.0 grams for the compliant clutch with centrifugal throw-out and the compliant clutch without throw-out, respectively. The introduction of compliance results in a savings of 2.31% in weight for the clutch with throw-out and a savings of 5.66% in weight for the clutch without throw-out. Although these amounts do not appear to be very significant, they may result in large savings in material costs if large volumes are manufactured.

7.5 Fatigue

In the previous chapter fatigue predictions were made for the steel and the aluminum compliant clutches. For the rigid-body clutch, the maximum bending stress of the leaf beam was calculated for a steel clutch and an aluminum clutch. The maximum stresses are 14400 lb./in.² for the aluminum clutch and 31600 lb./in.² for the steel clutch. Using the same fatigue-strength diagram for 7075-T6 Aluminum found in Juvinall, 1967, the predicted fatigue life for the rigid-body clutch is also in excess of 1.0×10^9 cycles. The stress in the rigid-body clutch is also 39% less than the maximum stress in the compliant aluminum clutch. This indicates that the traditional clutch should have a large safety factor in fatigue. The maximum bending stress in the rigid-body steel clutch was compared to the endurance limit of 33150 lb./in.² that was calculated in the previous chapter. The comparison shows that the leaf spring in the traditional clutch should have infinite life, which is much better than the predicted fatigue life of the compliant clutch. The stress in the rigid-body clutch is 29% less than the maximum stress in the compliant clutch. This also indicates that the rigid-body clutch will perform better in fatigue and also has a higher safety

factor than its steel compliant counterpart. This result was expected due to the different constraints on the two clutches. The CCrat-pawl beam is modeled by an initially curved cantilever beam fixed at one end fixed in the y -direction at the other end, while the traditional clutch beam is modeled as a simple end-loaded cantilever beam.

Based on the comparison criteria, the compliant over-running ratchet and pawl clutch equals and out performs the traditional rigid-body ratchet and pawl clutch in many areas. The biggest weakness of the compliant ratchet and pawl clutch is its fatigue strength. The compliant clutch falls short of the performance of the traditional clutch for a given set of criteria. The compliant clutch design may be modified for infinite life, but if the same modifications were applied to a rigid-body clutch, it would still outperform the compliant one in fatigue.

Microelectromechanical Systems

Microelectromechanical systems (MEMS) are devices constructed using IC-type processes at the micro level and include both mechanical and electrical components. Madou, 1997, provides a discussion of several different microfabrication processes used to manufacture MEMS. These devices may be on the order of 10's of microns to 1-2 millimeters in size. Much of the MEMS technology is new and is still being developed. Considerable work has been done in the area of pressure and acceleration sensors, micro valves, micro motors, and in other areas. An interesting area in MEMS research is actuation methods which include electrostatic, magnetic, mechanic, optical, fluidic and thermal energy (Ananthasuresh and Kota, 1995).

A device such as a micro compliant over-running clutch could be useful in power transmission and for use in mechanical actuation. The indexing capability of the over-running clutch could possibly be used to turn intermittent rotary motion into linear motion which could then be used for actuation. The use of compliance in the clutch is attractive for MEMS applications because many of the micro-machining processes used to fabricate MEMS devices do not allow for any type of assembly at all. Also, there are fewer toler-

ance, wear, lubrication and backlash issues in compliant mechanisms (Ananthasuresh and Kota, 1995; Howell and Midha, 1997). This aids in increasing the precision of the mechanism also.

8.1 Micro Compliant Ratchet and Pawl Clutches

In this brief investigation, two micro compliant clutches were designed and fabricated using the MUMPs process by MCNC, Mehregany and Dewa, 1993, to determine if these clutches would function as they do at the macro level. The first design is a CCrat-pawl clutch type and the second design is a compliant clutch that loads the cantilever pawls in compression. Currently there does not exist a way to measure the output and free-wheeling torques of the clutches.

8.1.1 Micro Compliant Clutch Design 1

Figure 8-1 shows a micro compliant over-running ratchet and pawl clutch manufactured using the MUMPs micromachining process. The MUMPs process is a three layer micromachining process. The basic process consists of first depositing a layer of polycrystalline silicon (polysilicon). The wafer is then coated with photoresist. After the photoresist is patterned and developed, the polysilicon is etched. A layer of oxide is deposited to separate the first and second layers of polysilicon. Finally, the second layer of polysilicon is then deposited and the process is repeated.

The clutch is made out of polysilicon. The pawls are pinned to the substrate and the outer hub is also anchored to the substrate. The ratchet gear is also pinned to the

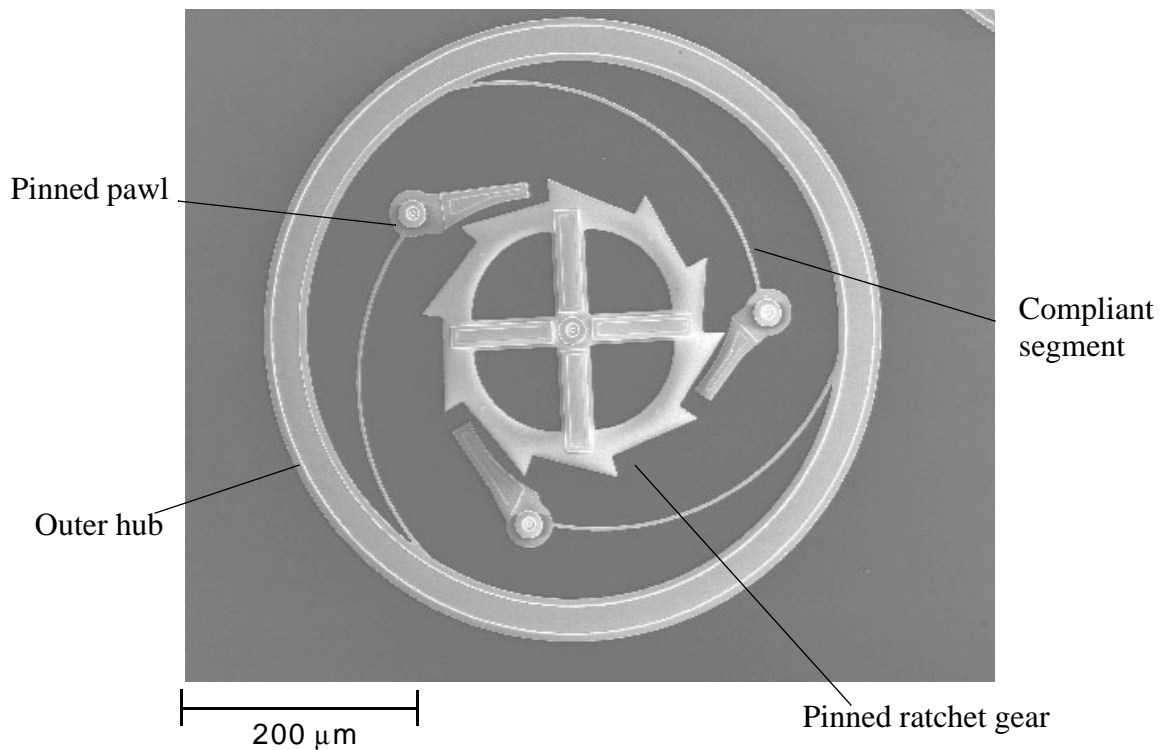


Figure 8-1 An SEM photo of a micro compliant over-running ratchet and pawl clutch.

substrate and allowed to rotate. The compliant segments were designed using the minimum allowable line width of $3.0\ \mu\text{m}$. The outer hub of the clutch is $480\ \mu\text{m}$ in diameter. The entire clutch hub is $1.5\ \mu\text{m}$ thick.

The clutch was tested to show that a compliant over-running ratchet and pawl clutch is feasible at the micro scale and merits further research. The clutch was actuated under a microscope using probe tips to rotate the ratchet gear in the free-wheeling and torque output directions. In testing, the clutch rotated freely in the over-running direction and engaged in the torque output direction. However, it was easy to apply a large enough torque to cause the clutch to fail.

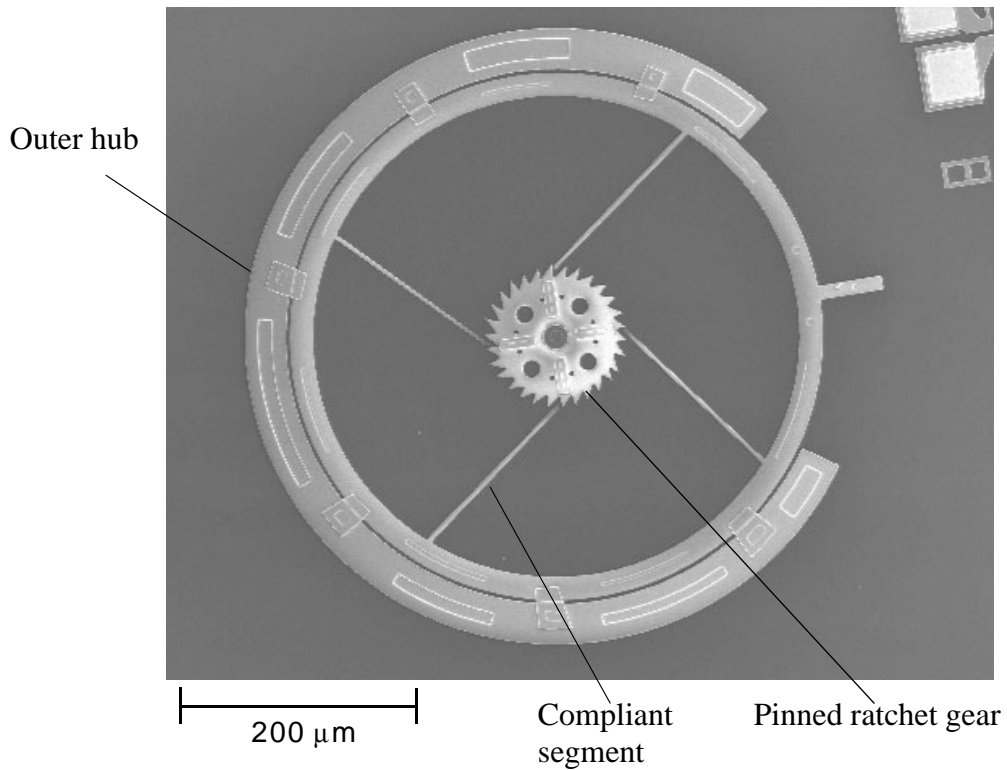


Figure 8-2 A micro compliant ratchet and pawl clutch with the pawls loaded in compression.

8.1.2 Micro Compliant Clutch Design 2

The second clutch design uses a cantilever beam for the pawl that is loaded in compression in the torque output direction and bending in the free-wheeling direction. The outer hub is free to rotate within the outer socket which is anchored to the substrate. The ratchet gear is pinned to the substrate and is allowed to rotate freely in the torque output direction. The ratchet has enough friction to keep it from rotating when the outer hub rotates in the free-wheeling direction. The pawls are 160 μm in length and 3 μm in width.

The outer radius of the clutch hub is 260 μm . The entire clutch hub is 1.5 μm thick. This clutch was manufactured using the same process described above.

The clutch was tested using the same probe tips as the previous clutch. In testing, this clutch did not perform as well as the CCrat-pawl clutch. The pawls buckled and fractured with little force being applied in the torque output direction.

The micro CCrat-pawl clutch was demonstrated to be a feasible device that is worthy of further research and investigation. The clutch has a possible application for use in actuation at the micro level.

9.1 Conclusions

The majority of the conclusions of this research are based on the testing and analysis of six over-running ratchet and pawl clutch designs.

1. For over-running clutches the clutch type that best lends itself to the use of compliance is the ratchet and pawl type clutch.
2. To get the largest amount of output torque from the clutch, the pawls should be rigid members loaded in compression.
3. The pseudo-rigid body model is a valuable design tool for compliant mechanism synthesis.
4. Compliant mechanism theory can be used in over-running clutch design to design clutches with fewer parts and lower manufacturing and assembly costs. Also, the clutches designed using this theory perform very comparable to traditional rigid-body ratchet and pawl clutches.

5. The developed theory can be applied to several material types and can also be used to design functional clutches at the micro level.

9.2 Recommendations for Further Research

The purpose of this research was to investigate over-running clutches designed using compliant mechanism theory. In this investigation the entire design space for ratchet and pawl clutches was not completely explored, and several areas exist in which further research may be done to strengthen and build on the conclusions of this research. Some of these possible areas include:

1. In the preliminary design of different types of compliant ratchet and pawl clutches, the tension design using small-length flexural pivots produced promising results. This is an area where further research may be done to increase the output torque of the clutch.

2. In the determination of which clutch type is best for the use of compliance, the sprag type clutch was shown to be a possible candidate for the use of compliance. Further research would be required. One possible idea is to use sprags attached to initially curved compliant segments that are attached to the hub and provide the spring force to keep the sprags in the proper position for friction engagement of the clutch.

3. An investigation into inversion designs of ratchet and pawl clutches in compression where the pawls are attached to the ratchet instead of the hub. This may be a way to reduce backlash and to reduce the overall size of the clutch.

4. Further research is needed in the area of clutch fatigue. Full scale testing would provide much needed information on polymer designs and clutch dynamic and fatigue failure modes.

5. Because the field of MEMS is such a new and growing field, much research can be done with micro compliant over-running clutches for possible applications in indexing and actuation methods.

REFERENCES

Ananthasuresh, G.K., Kota, S., Crary, S.B., Wise, K.D., 1992, "Design and Fabrication of Microelectromechanical Systems," *Proceedings of the 1992 ASME Mechanisms Conference*, DE-Vol. 45, pp. 251-258.

Ananthasuresh, G.K., Kota, S. and Gianchandani, Y., 1993, "Systematic Synthesis of Microcompliant Mechanisms - Preliminary Results," *Proceedings of the Third National Applied Mechanisms and Robotics Conference*, Cincinnati, Ohio, Paper No. AMR-93-082.

Ananthasuresh, G.K., 1994, "A New Design Paradigm for Micro-Electro-Mechanical Systems & Investigations on the Compliant Mechanism Synthesis," Dissertation, University of Michigan, Ann Arbor, Michigan.

Ananthasuresh, G.K., Kota, S. and Gianchandani, Y., 1994, "A Methodical Approach to the Design of Compliant Mechanisms," *Solid-State Sensor and Actuator Workshop*, Hilton Head Island, South Carolina, pp. 189-192.

Ananthasuresh, G.K., and Kota, S., 1995, "Designing Compliant Mechanisms," *Mechanical Engineering*, Vol. 117, No. 11, pp. 93-96.

Ananthasuresh, G.K., and Kota, S., 1996, "The Role of Compliance in the Design of MEMS," *Proceedings of the 1996 ASME Design Engineering Technical Conferences*, 96-DETC/MECH-1309.

Bickford, J.H., 1968, "12 Ways to go 1 Way," *Machine Design*, Vol. 40, No. 18, pp. 112-115.

Bisshopp, K.E. and Drucker, D.C., 1945, "Large Deflection Of Cantilever Beams," *Quarterly of Applied Mathematics*, Vol. 3, No. 3, pp. 272-275.

Boronkay, T.G., and Mei, C., 1970, "Analysis and Design of Multiple Input Flexible Link Mechanisms," *Journal of Mechanisms*, Vol. 5, No. 1, pp. 29-49.

Burns, R.H., 1964, "The Kinetostatic Synthesis of Flexible Link Mechanisms," Ph.D. Dissertation, Yale University, New Haven, Connecticut.

Burns, R.H., and Crossley, F.R.E., 1966, "Structural Permutations of Flexible Link Mechanisms," ASME Paper No. 66-MECH-5.

Burns, R.H., and Crossley, F.R.E., 1968, "Kinetostatic Synthesis of Flexible Link Mechanisms," ASME Paper No. 68-MECH-36.

- Burstall, A.F., 1963, *A History of Mechanical Engineering*, Pitman Publishing Corporation, New York, New York.
- Chironis, N.P., Rossner, E.E., 1991, *Mechanisms & Mechanical Devices Sourcebook*, McGraw-Hill Inc., New York.
- Coulter, B.A. and Miller, R.E., 1988, "Numerical Analysis of a Generalized Plane 'Elastica' with Non-Linear Material Behavior," *International Journal for Numerical Methods in Engineering*, Vol. 26, pp. 617-630.
- Daniels, R. L., 1967, "Design and Performance Characteristics of Over-Running Clutches in Gas Turbine Drive Applications," *Machine Design*, Volume 39, 1967, pp. 207-215.
- Derderian, J.M., Howell, L.L., Murphy, M.D., Lyon, S.M., and Pack, S.D., 1996, "Compliant Parallel-Guiding Mechanisms," Proceedings of the 1996 ASME DEsign Engineering Technical Conferences, 96-DETC/MECH-1208.
- Derderian, J.M., 1996, "The Pseudo-Rigid-Body-Model Concept and Its Application to Micro Compliant Mechanisms," M.S. Thesis, Brigham Young University, Provo, Utah.
- Edwards, B.T., 1996, "Functionally Binary Pinned-Pinned Segments," M.S. Thesis, Brigham Young University, Provo, Utah.
- Forbes, R.J., 1958, *A History of Technology*, Volume 4, Oxford University Press, New York, New York.
- Frecker, M.I., Kota, S., Fonseca, J., and Kikuchi, N., 1995, "A Systematic Synthesis Method for the Design of Distributed Compliant Mechanisms," *AMR '95 - The Fourth National Applied Mechanisms and Robotics Conference*, Cincinnati, OH, Vol.2 #062, December, 1995.
- Frecker, M.I., Kikuchi, N., and Kota, S., 1996, "Optimal Synthesis of Compliant Mechanisms to Meet Structural and Kinematic Requirements-Preliminary Results," *Proceedings of the 1996 ASME Design Engineering Technical Conferences*, 96-DETC/DAC-1497.
- Frecker, M.I., Kota, S., Kikuchi, N., 1997, "Use of Penalty Function in Topological Synthesis and Optimization of Strain Energy Density of Compliant Mechanisms," *Proceedings of DETC'97 1997 ASME Design Engineering Technical Conferences*, DETC97/DAC-3760.
- Frisch-Fay, R., 1962, *Flexible Bars*, Butterworth, Washington, D.C.
- Gandhi, M.V. and Thompson, B.S. 1980, "The Finite Element Analysis of Flexible Components of Mechanical Systems Using a Mixed Variational Principle," ASME Paper No. 80-DET-04.

Her, I., Midha, A., Salamon, B.A., 1992, "A Methodology for Compliant Mechanisms Design: Part II - Shooting Method and Application," *Advances in Design Automation*, (Ed.: D.A. Hoeltzel), DE-Vol.44-2, 18th ASME Design Automation Conference, pp. 39-45.

Hill, T.C., and Midha, A., 1990, "A Graphical User-Driven Newton-Raphson Technique for use in the Analysis and Design of Compliant Mechanisms," *Journal of Mechanical Design*, Trans. ASME, Vol. 112, No. 1, pp. 123-130.

Hilliard Corporation, 1997, <http://www.hilliardcorp.com/images/sprag.jpg>.

Howell, L.L., 1991, "The Design and Analysis of Large-Deflection Members in Compliant Mechanisms," M.S. Thesis, Purdue University, West Lafayette, Indiana.

Howell, L.L., and Midha, A., 1994, "A Method for the Design of Compliant Mechanisms with Small-Length Flexural Pivots," *ASME Journal of Mechanical Design*, Vol. 116, No. 1, pp. 280-290.

Howell, L.L., and Midha, A., 1995, "Parametric Deflection Approximations for End-Loaded, Large-Deflection Beams in Compliant Mechanisms," *ASME Journal of Mechanical Design*, Vol. 117, No.1, pp. 156-165.

Howell, L.L., Midha, A., Norton, T.W., 1996, "Evaluation of Equivalent Spring Stiffness for Use in a Pseudo-Rigid-Body Model of Large-Deflection Compliant Mechanisms," *ASME Journal of Mechanical Design*, Vol. 118, No. 1, pp. 126-131.

Howell, L.L., and Midha, A., 1996, "Parametric Deflection Approximations for End-Loaded, Large-Deflection Beams in Compliant Mechanisms," *Proceedings of the 1996 ASME Design Engineering Technical Conferences*, 96-DETC/MECH-1215.

Howell, L.L., and Leonard, J.N., 1997, "Optimal Loading Conditions for Non-Linear Deflections," *International Journal of Non-Linear Mechanics*, Vol. 32, No. 3, pp. 505-514.

Howell, L.L., and Midha, A., 1997, "Compliant Mechanisms," Notes for MeEn 538, Brigham Young University, Provo, Utah.

Jensen, B.D., Howell, L.L., Gunyan, D.B., Salmon, L.G., 1997, "The Design and Analysis of Compliant MEMS Using the Pseudo-Rigid-Body Model," *Proceedings of the 1997 International Mechanical Engineering Congress & Exposition*.

Juvinall, R.C., 1967, *Stress, Strain, and Strength*, McGraw-Hill Book Company, New York, New York.

- Kota, S., Ananthasuresh, G.K., Crary, S.B., Wise, K.D., 1994, "Design and fabrication of Microelectromechanical Systems," *ASME Journal of Mechanical Design*, Vol. 116, pp. 1081-1088.
- Kragelsky, I.V., Dobychn, M.N., and Kombalov, V.S., 1982, *Friction & Wear Calculation Methods*, Pergamnon Press, New York, New York.
- Larsen, V.D., Sigmund, O., and Bouwstra, S., 1996, "Design and Fabrication of Compliant Micromechanisms and Structures with Negative Poisson's Ratio," *Proceedings of the Ninth Annual International Workshop on Micro Electro Mechanical Systems*, San Diego, CA, February 11-15, pp. 365-371.
- Lewis, G. and Monasa, F., 1981, "Large Deflections of Cantilever Beams of Nonlinear Materials," *Computers and Structures*, Vol. 14, No. 5-6, pp. 357-360.
- Lowery, R. D. and Mehrbrodt, A. W., 1976, "How to do More With Wrapped-Spring Clutches," *Machine Design*, Volume 48, Number 17, pp. 78-83.
- Madou, M., 1997, *Fundamentals of Microfabrication*, CRC Press, New York, New York.
- Mattiasson, K., 1981, "Numerical results from Large Deflection Beam and Frame Problems Analyzed by Means of Elliptic Integrals," *International Journal for Numerical Methods in Engineering*, Vol. 17, pp. 145-153.
- Mehregany, M. and Dewa, A.S., 1993, *Case Western Reserve University - MCNC Short Course Handbook: Introduction to Microelectromechanical Systems and the Multiuser MEMS Processes*, Electronics Design Center and Department of Electrical Engineering and Applied Physics, Case Western Reserve University, Cleveland, Ohio.
- Mettlach, G.A., and Midha, A., 1996, "Using Burmester Theory in the Design of Compliant Mechanisms," *Proceedings of the 1996 ASME Design Engineering Technical Conferences*, 96-DETC/MECH-1181.
- Midha, A., Her, I., Salamon, B.A., 1992, "A Methodology for Compliant Mechanisms Design: Part I - Introduction and Large-Deflection Analysis," *Advances in Design Automation*, (Ed.: D.A. Hoeltzel), DE-Vol.44-2, 18th ASME Design Automation Conference, pp. 29-38.
- Midha, A., Norton, T.W., and Howell, L.L., 1994, "On the Nomenclature, Classification, and Abstractions of Compliant Mechanisms," *ASME Journal of Mechanical Design*, Vol. 116, No. 1, pp. 270-279.
- Miller, R.E., 1980, "Numerical Analysis of a Generalized Plane Elastica," *International Journal for Numerical Methods in Engineering*, Vol. 15, pp. 325-332.

Norton, T.W., 1991, "On the Nomenclature and Classification, and Mobility of Compliant Mechanisms," M.S. Thesis, Purdue University, West Lafayette, Indiana.

Orthwein, W.C., 1986, *Clutches and Brakes Design and Selection*, Marcel Dekker, Inc., New York, New York.

Parkinson, M.B., Howell, L.L., Cox, J.J., "A Parametric Approach to the Optimization-Based Design of Compliant Mechanisms," *Proceedings of 1997 Design Engineering Technical Conferences*, DETC97/DAC-3763.

Schwinn, F.W., 1945, *50 Years of Schwinn-Built Bicycles*, Arnold, Schwinn & Company, Chicago, Illinois.

Sevak, N.M., and McLarnan, C.W., 1974, "Optimal Synthesis of Flexible Link Mechanisms with Large Static Deflections," ASME Paper No. 74-DET-83.

Shoup, T.E., 1972, "On the Use of the Nodal Elastica for the Analysis of Flexible Link Devices," *Journal of Engineering for Industry*, Trans. ASME, Vol. 94, No. 3, pp. 871-875.

Shoup, T.E., and McLarnan, C.W., 1971, "On the Use of the Undulating Elastica for the Analysis of Flexible Link Mechanisms," *Journal of Engineering for Industry*, Trans. ASME, pp. 263-267.

Smith, C.G. and Rees, G., 1978, *The Inventions of Leonardo Da Vinci*, Phaidon Press Limited, Oxford, England.

South, D.W. and Mancuso, J.R., 1994, *Mechanical Power Transmission Components*, Marcel Dekker, Inc., New York, New York.

Stieber, 1997, <http://www.riv.org/stieber.htm>.

Wiebusch, C. F., 1939, "The Spring Clutch," *Journal of Applied Mechanics*, Volume 6, pp. 103-108.

Young, W.C., 1989, *Roark's Formulas for Stress & Strain*, McGraw-Hill Book Company, New York, New York.

Xu, T. and Lowen, G. G., 1994, "A Mathematical Model of an Over-Running Sprag Clutch," *Mechanism and Machine Theory*, Volume 29, number 1, pp. 11-23.

APPENDIX A

Finite element model batch file ran on ANSYS

```
/BATCH
/COM,ANSYS REVISION 5.2  UP121895      09:12:51  03/23/1998
ll=1.439
rr=1.96
hh=.004
bb=.25
lr=.25
hr=.25
ex=30.0e6
ldiv=20
ldivr=5
rot1=-.149
rot2=-.16
/PREP7
ET,1,BEAM3
R,1,bb*hh,bb*(hh**3)/12,hh,1.2, , ,
R,2,hr*bb,bb*(hr**3)/12,hr,1.2,0,0,
UIMP,1,EX, , ,ex,
UIMP,1,NUXY, , ,0.3,
UIMP,1,EMIS, , ,1,
k,1,0,0
k,2,ll,0
k,3,-lr,0
k,4,ll/2,-rr/5
larc,1,2,4,rr
esize,,ldiv
l,1,3
real,1
type,1
mat,1
lmesh,1
esize,,ldivr
real,2
lmesh,2
FINISH
/SOLU
NLGEOM,1
NROPT,AUTO, ,
```

```

LUMPM,0
EQLV,FRONT,1e-08,0,
SSTIF
PSTRES
TOFFST,0,
dk,2,all,0
/com,dk,3,ux,0
dk,3,uy,0
dk,3,rotz,rot1
lswrite,1
dk,3,rotz,rot2
lswrite,2
lssolve,1,2
FINISH
/POST1
ksel,s,kp,,3
nslk,s
*get,nkp3,node,0,num,max
ksel,all
nset,all
set,1
ETABLE,smxi,NMIS,1
ETABLE,smxj,NMIS,3
ETABLE,smni,NMIS,2
ETABLE,smnj,NMIS,4
esort,etab,smxi,0,0
*get,smx1,sort,0,max
esort,etab,smni,0,0
*get,smn1,sort,0,min
eusort
set,2
ETABLE,smxi,NMIS,1
ETABLE,smxj,NMIS,3
ETABLE,smni,NMIS,2
ETABLE,smnj,NMIS,4
esort,etab,smxi,0,0
*get,smx2,sort,0,max
esort,etab,smni,0,0
*get,smn2,sort,0,min
eusort
fini
/POST26
nsol,2,nkp3,rot,z,rotz
rforce,3,nkp3,m,z,mz
/output,output
*stat

```

```
prvar,2,3  
/output  
save  
fini
```